View metadata, citation and similar papers at core.ac.uk
brought to you by CORE
provided by OTHES

MASTERARBEIT

Titel

Rotating Bose-Einstein Condensates in Partially Anisotropic Traps

Verfasser

BSc Thomas Auzinger

angestrebter akademischer Grad

Master of Science (MSc)

Wien, 30.03.2010

Studienkennzahl:	A 066 876
Studienrichtung:	Masterstudium Physik
Betreuer:	O. Univ. Prof. Dr. Jakob Yngvason

1 Abstract — Zusammenfassung

We study three-dimensional rapidly rotating Bose-Einstein condensates in a theoretical context. The main results are lower and upper bounds on the Gross-Pitaevskii energy of the dilute Bose gas in the Thomas-Fermi limit. Similar results were already obtained for strongly anharmonic external potentials in 2D [CRDY07b, CY08] and homogeneous external potentials in 2D [CRDY07a] and 3D [BCPY08] whereas we present the treatment of partially anisotropic traps in 3D. Furthermore a complete description and illustration of the Thomas-Fermi density in this limit is given. We also supply the source code for the generation of the illustrations.

Wir untersuchen dreidimensionale schnell rotierende Bose-Einstein Kondensate in einem theoretischen Kontext. Die Hauptresultate sind untere und obere Schranken an die Gross-Pitaevskii Energie des verdünnten Bose Gases im Thomas-Fermi Limes. Ähnliche Resultate wurden bereits für stark anharmonische äußere Potentiale in 2D [CRDY07b, CY08] und homogene äußere Potentiale in 2D [CRDY07a] und 3D [BCPY08] entwickelt wohingegen wir die Betrachtung von teilweise anisotropen Fallen in 3D präsentieren. Weiters geben wir eine komplette Beschreibung und Illustration der Thomas-Fermi Dichte in diesem Grenzwert an. Wir stellen auch den Quelltext zur Erstellung der Illustrationen zur Verfügung.

Contents

1 Abstract — Zusammenfassung **1**

2 Introduction **5**

3 General Setting **7**
3.1 The Hamiltonian . . . 7
3.2 The Gross-Pitaevskii (GP) Functional . . . 8
3.3 The Scalings of the GP Functional . . . 9

4 The Thomas-Fermi (TF) Framework **12**
4.1 Scaling of the TF Functional . . . 12
4.2 The Support of the TF Densities . . . 13
4.3 The Behavior of the Support near $z = 0$ . . . 15
4.4 Explicit Calculations of the TF Densities . . . 16
4.4.1 The Non-Rotational Case, $\Omega = 0$ . . . 16
4.4.2 The Emergence of a 'hole', $\mu_{1,\omega}^{\mathrm{TF}} = 0$ . . . 17
4.4.3 The General Case . . . 17
4.5 Limit of the TF Density as $\omega \to \infty$ ($\gamma \to \mathbf{0}$) . . . 18
4.6 Illustrations of the TF Density . . . 20

5 The TF Limit of the GP Functional **24**
5.1 TF Limit for $\omega < \infty$ . . . 24
5.2 The Electrostatic Analogy . . . 33
5.3 TF Limit for $\omega \to \infty$ . . . 36

A Source code **39**
A.1 $\omega < \infty$ . . . 39
A.2 $\omega \to \infty$ . . . 42

B Acknowledgments **45**

References **46**

> [I]f in other sciences we should arrive at certainty without doubt and truth without error, it behooves us to place the foundations of knowledge in mathematics, in so far as disposed through it we are able to reach certainty in other sciences and truth by the exclusion of error.
>
> Roger Bacon[1]

2 Introduction

The underlying topic of this thesis are Bose-Einstein condensates (BECs), named after Satyendra Nath Bose and Albert Einstein. The first step toward their prediction was done by Bose in 1924, who found out that a new kind of particle statistics enable him to derive Planck's law of radiation without any reference to classical physics. At first rejected by journals he was able to publish this seminal work with the help of Albert Einstein [Bos24]. His work was then generalized by Einstein who discovered that an ideal gas, which is governed by Bose-Einstein statistics, would condense into the lowest accessible quantum state when sufficiently cooled [Ein25]. This process was later named Bose-Einstein condensation. While theoretically compelling, an experimental validation of the theory took 70 years due to the technical difficulties that had to be mastered. A partial result was already obtained in 1938 when Pjotr L. Kapitza [Kap38], John F. Allen and Don Misener [AM38] discovered superfluidity in helium-4 at temperatures less than 2.17K. It already showed typical properties of a BEC such as vanishing viscosity and quantized vortices when being rotated but the strong interactions between the liquid's particles prevented a full condensation. Only around 10% of the atoms are in the ground state [Lon38, PO56, SS95].

In 1995 the realization of a true BEC was obtained as the goal in a race between the experimental groups around Eric Cornell and Carl Wiedman at the Boulder NIST-JILA lab [AEM+95] and Wolfgang Ketterle at MIT [DMA+95]. Cornell and Wiedman achieved the condensation of approximately 2000 ^{87}Rb atoms at temperatures below 170nK while Ketterle obtained the condensation of approximately 10^5 ^{23}Na atoms two months later. Both used laser cooling and magnetic evaporation cooling to achieve such low temperature — technologies that had to be developed over the span of 70 years to allow such a feat. All three were awarded the Nobel Prize in Physics for their achievement in 2001 [CW02, Ket02].

Refinement of the experiments allowed the study of rotating BECs [MAH+99, MCWD00, CMD00, ARVK01] — the main interest of this thesis. Related areas of research are the 'bose-nova' — the spontaneous im- and explosion of a certain BEC [RCC+01] —, BECs consisting of molecules [JBA+03] or Cooper pairs [GRJ03], the drastic slowing down of light beams even so far as to temporarily stopping them [HHDB99, LDBH01] and the attempt to model black hole physics with vortices in rotating BECs [LIB+09, MP09].

The original theory of BECs was greatly expanded by the work of Bogoliubov on weakly interacting Bose gases [Bog47a, Bog47b] in 1947. By an approximation to the system's Hamiltonian he obtained the energy of the ground state. The usual framework in which condensates are theoretically examined was developed by Gross [Gro61, Gro63] and Pitaevskii [Pit61] and has at its core the Gross-Pitaevskii (GP) energy functional [DGPS99] which has a non-linear cubic Schrödinger equation as its variational equation. Since this functional is evaluated on a single complex condensate wavefunction $\phi : \mathbb{R}^3 \to \mathbb{C}$ it is much easier to handle than the full many-particle Hamiltonian

[1] Translation by Robert Burke, Opus Majus of Roger Bacon (1928), vol 1, 124. In Fred R. Shapiro, The Yale Book of Quotations (2006), 39.

of the Bose gas and we will make great use of it in this work. A rigorous derivation of the GP framework from the full quantum-mechanical Hamiltonian with repulsive particle interactions was done for systems at rest [LSY00] and rotating systems [LS06] by Elliot Lieb, Robert Seiringer and Jakob Yngvason. For an overview of the mathematical modeling of BECs we refer to the works of Amandine Aftalion [Aft07] and Alexander L. Fetter [Fet09].

For condensates that are trapped by an external potential that grows faster than harmonic it is theoretically possible to rotate the condensate arbitrarily fast without losing the confinement. The mathematical treatment of such cases was already done for strongly anharmonic traps in 2D [CRDY07b, CY08] and homogeneous traps in 2D [CRDY07a] and 3D [BCPY08] by Michele Correggi, Tanja Rindler-Daller, Jean-Bernard Bru, Peter Pickl and Jakob Yngvason. In this thesis we will extend this field by the treatment of partially anisotropic potentials of the form $r^s + |z|^t$ with $s > 2$ and $t > 0$.

If one takes a harmonic trap several new features arise. At first there exists a critical angular velocity which is the fastest a condensate can rotate without flying apart. Close to this limit one finds an analogy to theory of Lowest Landau Levels of charged particles in magnetic fields. This regime is an active field of research and there exist predictions that for high angular momenta new effects such as similarities to the Fractional Quantum Hall Effect or the emergence of anyonic and perhaps non-abelian particle statistics can be found. We refer to the review article by Nigel R. Cooper for an overview [Coo08].

3 General Setting

3.1 The Hamiltonian

We start with the Hamiltonian of N interacting bosonic particles given by the operator[2]

$$H_N \equiv \sum_{i=1}^{N} H_0^{(i)} + \sum_{1\leq i<j\leq N} v(\vec{x}_i - \vec{x}_j), \qquad \vec{x}_i, \vec{x}_j \in \mathbb{R}^3 \tag{3.1}$$

acting on the symmetric product of Hilbert spaces of wave functions, i.e., $L^2(\mathbb{R}^3)^{\otimes_s N}$. $H_0^{(i)}$ denotes the one-body Hamiltonian of particle i and will be defined below. The interaction is modeled by the two-particle interaction potential v. We demand v to be spherically symmetric ($v(\vec{x}) = v(|\vec{x}|)$), non-negative and of finite range ($\exists R > 0$ such that $v(\vec{x}) = 0$ for $|\vec{x}| > R$). This yields a repulsive two-body interaction which can be assigned a characteristic parameter of the interaction.

The *scattering length* α of a potential $\nu(|\vec{x}|)$ with finite range R is defined as follows: The solution $\Psi(\vec{x})$ of the zero energy scattering Schrödinger equation

$$-\Delta\Psi(\vec{x}) + \tfrac{1}{2}\nu(|\vec{x}|)\Psi(\vec{x}) = 0$$

with the boundary condition $\Psi(\vec{x}) \to 1$ as $|\vec{x}| \to \infty$ has the form

$$\Psi(\vec{x}) = 1 - \frac{\alpha}{|\vec{x}|} \qquad \text{for } |\vec{x}| > R$$

which we use as the definition of the scattering length α.

Since we are interested in a description of spinless bosons in a rotating external trap we define the one-body Hamiltonian in the rotating frame as

$$H_0 = -\Delta + \vec{L}\cdot\vec{\Omega} + V(\vec{x}) \tag{3.2}$$

where $\vec{L} = i(\vec{\nabla}\times\vec{x})$ is the angular momentum operator and $\vec{\Omega}$ denotes the angular velocity of the rotating trapping potential V. As we model identical particles each one-body Hamiltonian $H_0^{(i)}$ in (3.1) is given by H_0. We assume uniform particle mass m and scale our units for convenience such that $2m = \hbar = 1$. We fix the axis rotation as the z-axis, i.e., $\vec{\Omega} = (0, 0, \Omega) = \Omega\vec{e}_z$ with the scalar angular velocity Ω. It is convenient to add and subtract the term $\frac{1}{2}(\Omega\times\vec{x})$ to H_0 so that it can be rewritten by completion of the square as

$$H_0 = \left(-i\vec{\nabla} - \vec{A}_\Omega(\vec{x})\right)^2 + V(\vec{x}) - \tfrac{1}{4}\Omega^2 r^2 \tag{3.3}$$

with $r = |\vec{r}\,| = |\vec{x}\times\vec{e}_z|$ and a vector potential $\vec{A}_\Omega(\vec{x}) \equiv \frac{1}{2}\Omega(\vec{e}_z\times\vec{x})$. The vector potential can be thought of as the 'Coriolis force' in the rotating frame and is the main reason for the formation of vortices.

The choice of the external potential is now a fundamental aspect of this thesis as it determines the special case for which we calculate the ground state energy asymptotics. In general, V has to be bounded from below and has to be confining in the sense that $V(\vec{x}) \to \infty$ as $|\vec{x}| \to \infty$ to render the Hamiltonian sufficiently well behaved. Since we are interested in limits of large angular velocity Ω the external potential must not be overwhelmed by the centrifugal 'force' $\Omega^2 r^2$. All these requirements are met by our choice of an *anisotropic external potential*

$$V(\vec{x}) \equiv r^s + |z|^t, \qquad s > 2, t > 0.$$

In radial direction this potential grows faster than harmonic and thus our system does not fly apart at arbitrarily high angular velocities Ω.

[2]For vectors in $\mathbb{R}^3$ we use the notation $\vec{x} = (x, y, z) = (\vec{r}, z)$ throughout this thesis.

3.2 The Gross-Pitaevskii (GP) Functional

The GP energy functional of a function ϕ in the rotating frame is given by

$$\begin{aligned} E^{\mathrm{GP}}_{g,\Omega}[\phi] &\equiv \langle \phi | H_0 | \phi \rangle + g \int_{\mathbb{R}^3} \mathrm{d}\vec{x}\, |\phi|^4 \\ &= \int_{\mathbb{R}^3} \mathrm{d}\vec{x} \left\{ \left| \left(\vec{\nabla} - i\vec{A}_\Omega \right) \phi \right|^2 + \left(r^s + |z|^t \right) |\phi|^2 - \tfrac{1}{4}\Omega^2 r^2 |\phi|^2 + g|\phi|^4 \right\} \end{aligned}$$

with the GP parameter

$$g \equiv 4\pi a N \tag{3.4}$$

and defined on the domain of functions from $\mathbb{R}^3$ to $\mathbb{C}$

$$\mathcal{D}^{\mathrm{GP}} \equiv \left\{ \phi : \phi \in L^2(\mathbb{R}^3) \cap L^4(\mathbb{R}^3), \vec{\nabla}\phi \in L^2(\mathbb{R}^3), \left(r^s + |z|^t \right) \phi \in L^1(\mathbb{R}^3) \right\}.$$

We have omitted the argument $(\vec{x})$ of both $\vec{A}_\Omega$ and ϕ for convenience and will continue to do so. We will be interested in the lowest attainable energy of this functional, i.e.,

$$E^{\mathrm{GP}}_{g,\Omega} \equiv \inf_{\phi \in \mathcal{D}^{\mathrm{GP}}, \|\phi\|_2 = 1} \mathcal{E}^{\mathrm{GP}}_{g,\Omega}[\phi]$$

which we call the *GP energy*. It can be shown that the infimum exists and is a minimum [LSY00]. We denote a corresponding minimizer by $\phi^{\mathrm{GP}}_{g,\Omega}$ such that $E^{\mathrm{GP}}_{g,\Omega} = \mathcal{E}^{\mathrm{GP}}_{g,\Omega}[\phi^{\mathrm{GP}}_{g,\Omega}]$. Note that such a minimizer is not necessarily unique in the rotating case [LS06]. Naturally it obeys the Euler Lagrange equation of the GP energy — the *GP equation* —

$$\left(-\left(\vec{\nabla} - i\vec{A}_\Omega \right)^2 + r^s + |z|^t - \tfrac{1}{4}\Omega^2 r^2 + 2g \left| \phi^{\mathrm{GP}}_{g,\Omega} \right|^2 \right) \phi^{\mathrm{GP}}_{g,\Omega} = \mu^{\mathrm{GP}}_{g,\Omega} \phi^{\mathrm{GP}}_{g,\Omega}. \tag{3.5}$$

The Lagrange multiplier $\mu^{\mathrm{GP}}_{g,\Omega}$ is called the *GP chemical potential* and given by

$$\mu^{\mathrm{GP}}_{g,\Omega} \equiv E^{\mathrm{GP}}_{g,\Omega} + g \int_{\mathbb{R}^3} \mathrm{d}\vec{x}\, \left| \phi^{\mathrm{GP}}_{g,\Omega} \right|^4.$$

It ensures the normalization of the minimizer in (3.5) and corresponds to the energy per particle to add a small number of particles to the system.

The GP functional was obtained by Gross [Gro61, Gro63] and Pitaevskii [Pit61] from the full quantum mechanical Hamiltonian by heuristic arguments. In recent years a strictly mathematical proof of the validity of such an approximation was given for an interacting Bose gas at rest [LSY00] and a rotating one [LS06]. The main results are limit theorems of the form

$$\lim_{N \to \infty} \frac{E^{\mathrm{QM}}(N, \Omega)}{N} = E^{\mathrm{GP}}_{g,\Omega}$$

with E^{QM} the ground state energy of a N-body Hamiltonian such as (3.1) and (3.2) in the sector of bosonic (symmetric) N-body wavefunctions. The GP parameter g is kept of order $O(1)$ in the limit $N \to \infty$. This immediately demands that the scattering length $a \propto g/N$ of the two-body interaction potential v of the Hamiltonian has to be of order $O(N^{-1})$. We can achieve such a behavior by setting $v(\vec{x}) = N^2 v_g(N\vec{x})$ with a fixed potential v_g. We call this the *GP limit* or *dilute limit* since the scattering length a of order $O(N^{-1})$ together with the mean GP density $\bar{\rho}$ of order $O(N)$ (see (3.6)) gives $a^3\bar{\rho} = O(N^{-2})$. The last term tells us that the interparticle distances become large with respect to the range of the interaction potential (given by the scatter length a) as $N \to \infty$.

The mean GP density for a given number of particles N is defined by

$$\bar{\rho} \equiv N \int_{\mathbb{R}^3} \mathrm{d}\vec{x} \, \left|\phi_{g,\Omega}^{\mathrm{GP}}\right|^4 . \tag{3.6}$$

Having outlined the fundamentals of the GP theory an essential clarification is still missing — the precise physical definition of Bose-Einstein condensation. We will give this shortly but need a definition in beforehand. Let Ψ be the normalized ground state wavefunction of the operator (3.1) with $\vec{\Omega} = \vec{0}$. We define the *one-particle density matrix* of Ψ as

$$\gamma(\vec{x}, \vec{x}') \equiv N \int_{\mathbb{R}^{3(N-1)}} \mathrm{d}\vec{X} \, \Psi(\vec{x}, \vec{X}) \Psi(\vec{x}', \vec{X})$$

where $\vec{X} \equiv (\vec{x}_2, \ldots, \vec{x}_N)$ and $\mathrm{d}\vec{X} \equiv \prod_{j=2}^{N} \mathrm{d}\vec{x}_j$. Complete Bose-Einstein condensation is then the property that in the limit of $N \to \infty$ the density matrix $\frac{1}{N}\gamma(\vec{x}, \vec{x}')$ becomes a product $\phi(\vec{x})\phi(\vec{x}')$ of a so-called *condensate wave function* ϕ.

It can be shown that in the GP limit ($N \to \infty$ with g fixed) on has full condensation of the many body ground state into the GP minimizer, i.e.

$$\lim_{N\to\infty} \frac{\gamma(\vec{x}, \vec{x}')}{N} = \phi_{g,0}^{\mathrm{GP}}(\vec{x}) \, \phi_{g,0}^{\mathrm{GP}}(\vec{x}') \tag{3.7}$$

where the limit is meant to be taken in the trace norm. This was proved by Elliot H. Lieb and Robert Seiringer [LS02] who also showed a similar result for the rotating case. In the latter case the solution of the GP equation is not generally unique and $\gamma(\vec{x}, \vec{x}')$ can not be assumed to be a pure state. It was then shown that the limit points of a set of approximate ground state is always a convex combination of projections onto the various GP minimizers. Due to technical details the precise statement is rather lengthy and we refer to [LS06, Thm. 2] for a rigorous definition.

3.3 The Scalings of the GP Functional

We are interested in the behavior of the GP energy and GP minimizer in the limit of rapid rotation. It is quiet clear that for a fixed external potential such a limit would cause the condensate to expand in all directions and become increasingly dilute. To counteract this process we will scale our coordinates according to the relation between g and Ω and between s and t. The exact nature of these scalings is the topic of this section.

Starting with the standard *GP functional* in the rotating frame

$$\mathcal{E}_{g,\Omega}^{\mathrm{GP}}[\phi] \equiv \int_{\mathbb{R}^3} \mathrm{d}\vec{x} \left\{ \left| \left(\vec{\nabla} - i\vec{A}_\Omega \right) \phi \right|^2 + \left(r^s + |z|^t \right) |\phi|^2 - \tfrac{1}{4}\Omega^2 r^2 |\phi|^2 + g|\phi|^4 \right\} \tag{3.8}$$

we scale both the radial and the z-direction independently. We set $\vec{r} \equiv \lambda \vec{r}'$ and $z \equiv \mu z'$ to get[3]

$$\begin{aligned} \mathcal{E}_{g,\Omega}^{\mathrm{GP}}[\phi] = \int_{\mathbb{R}^3} \mathrm{d}\vec{x}' \, \Bigg\{ & \left| \left(\lambda^{-1} \vec{\nabla}_{\vec{r}'} + \mu^{-1} \vec{\nabla}_{z'} - i\lambda \vec{A}_\Omega \right) \phi' \right|^2 \\ & + \left(\lambda^s r'^s + \mu^t \left|z'\right|^t \right) |\phi'|^2 - \tfrac{1}{4}\Omega^2 \lambda^2 r'^2 |\phi'|^2 + g\lambda^{-2}\mu^{-1} |\phi'|^4 \Bigg\} \end{aligned} \tag{3.9}$$

with

$$\phi'(\vec{r}\,', z') \equiv \lambda \mu^{1/2} \phi(\vec{r}, z)$$

[3] We use the abbreviation $\vec{\nabla}_{\vec{r}}$ for $(\partial_x, \partial_y, 0)$ and $\vec{\nabla}_z$ for $(0, 0, \partial_z)$.

by normalization. In the following investigations it will be necessary to differentiate two cases that depend on the general form of the external potential, which is determined by the exponents s and t. If $s > t$ the potential grows faster in radial direction than along the rotational axis. The relation $s < t$ gives the converse case. If the external potential is completely homogeneous ($V(\lambda\vec{x}) = \lambda^s V(\vec{x})$), thus $s = t$, the results of [BCPY08] can be applied. To make the notation more transparent, we will use the same letters for variables in both cases but with an underline for the case $s > t$ and an overline for $s < t$. In (3.9) we will set either

$$\mu = \lambda^{s/t} \quad \text{or} \quad \lambda = \mu^{t/s}.$$

Both choices ensure that the term of the external potential has only a single prefactor, which implies that its qualitative shape does not change with the scaling parameter. We arrive at

$$\begin{aligned}\mathcal{E}^{\mathrm{GP}}_{g,\Omega}[\phi] = \lambda^{-2} \int_{\mathbb{R}^3} \mathrm{d}\vec{x}' \, \Big\{ \Big| \Big(\vec{\nabla}_{\vec{r}'} + \lambda^{(t-s)/t} \vec{\nabla}_{z'} - i\vec{A}_{\lambda^2\Omega} \Big) \phi' \Big|^2 \\ + \lambda^{s+2} \Big(\Big(r'^s + |z'|^t \Big) |\phi'|^2 - \tfrac{1}{4}\Omega^2 \lambda^{2-s} r'^2 |\phi'|^2 + g\lambda^{-(s+(s+2)t)/t} |\phi'|^4 \Big) \Big\}\end{aligned} \tag{3.10}$$

and

$$\begin{aligned}\mathcal{E}^{\mathrm{GP}}_{g,\Omega}[\phi] = \mu^{-2} \int_{\mathbb{R}^3} \mathrm{d}\vec{x}' \, \Big\{ \Big| \Big(\mu^{(s-t)/s} \vec{\nabla}_{\vec{r}'} + \vec{\nabla}_{z'} - i\vec{A}_{\mu^{(s+t)/s}\Omega} \Big) \phi' \Big|^2 \\ + \mu^{t+2} \Big(\Big(r'^s + |z'|^t \Big) |\phi'|^2 - \tfrac{1}{4}\Omega^2 \mu^{-((s-2)t)/s} r'^2 |\phi'|^2 + g\mu^{-(s+(s+2)t)/s} |\phi'|^4 \Big) \Big\}.\end{aligned} \tag{3.11}$$

In the course of our examinations we will need an additional scaling depending on the relation between the rotational energy term $\propto \Omega^2 r'^2 |\phi'|^2$ and the interaction energy term $\propto g|\phi'|^4$. If the contribution to the total energy of the rotational term dominates it will be convenient to choose the scaling parameter λ and μ in a way such that the prefactor of the interaction term $|\phi'|^4$ is set to one, i.e., either $g\lambda^{-(s+(s+2)t)/t} = 1$ or $g\mu^{-(s+(s+2)t)/s} = 1$. This sets the scaling parameters to

$$\lambda \equiv g^{t/(s+(s+2)t)} \quad \text{or} \quad \mu \equiv g^{s/(s+(s+2)t)}. \tag{3.12}$$

To simplify the notation we will define additional variables $\underline{\varepsilon}$, $\bar{\varepsilon}$ and ω. In the case of $s > t$ we set

$$\underline{\varepsilon}^{-2} \equiv g^{(s+2)t/(s+(s+2)t)} = \lambda^{s+2} \tag{3.13}$$

and obtain the expression of the GP functional we will work with, namely,

$$\begin{aligned}\mathcal{E}^{\mathrm{GP}}_{g,\Omega}[\phi] &= \underline{\varepsilon}^{4/(s+2)} \int_{\mathbb{R}^3} \mathrm{d}\vec{x}' \, \Big\{ \Big| \Big(\vec{\nabla}_{\vec{r}'} + \underline{\varepsilon}^{\alpha} \vec{\nabla}_{z'} - i\vec{A}_{\omega/\underline{\varepsilon}} \Big) \phi' \Big|^2 \\ &\qquad + \underline{\varepsilon}^{-2} \Big(\Big(r'^s + |z'|^t \Big) |\phi'|^2 - \tfrac{1}{4}\omega^2 r'^2 |\phi'|^2 + |\phi'|^4 \Big) \Big\} \\ &\equiv \underline{\varepsilon}^{4/(s+2)} \mathcal{E}^{\mathrm{GP}}_{\underline{\varepsilon},\omega}[\phi']\end{aligned} \tag{3.14}$$

with $\alpha \equiv 2(s-t)/((s+2)t) > 0$. The case of $s < t$ leads to the definition

$$\bar{\varepsilon}^{\,-2} \equiv g^{s(t+2)/(s+(s+2)t)} = \mu^{t+2} \tag{3.15}$$

and the functional

$$\begin{aligned}\mathcal{E}^{\mathrm{GP}}_{g,\Omega}[\phi] &= \bar{\varepsilon}^{\,4/(t+2)} \int_{\mathbb{R}^3} \mathrm{d}\vec{x}' \, \Big\{ \Big| \Big(\bar{\varepsilon}^{\,\beta} \vec{\nabla}_{\vec{r}'} + \vec{\nabla}_{z'} - i\vec{A}_{\omega/\bar{\varepsilon}} \Big) \phi' \Big|^2 \\ &\qquad + \bar{\varepsilon}^{\,-2} \Big(\Big(r'^s + |z'|^t \Big) |\phi'|^2 - \tfrac{1}{4}\omega^2 r'^2 |\phi'|^2 + |\phi'|^4 \Big) \Big\} \\ &\equiv \bar{\varepsilon}^{\,4/(t+2)} \bar{\mathcal{E}}^{\mathrm{GP}}_{\bar{\varepsilon},\omega}[\phi']\end{aligned} \tag{3.16}$$

where $\beta \equiv 2(t-s)/(s(t+2)) > 0$. In both cases the parameter

$$\omega^2 \equiv \Omega^2 g^{-(s-2)t/(s+(s+2)t)} \tag{3.17}$$

denotes the strength of the rotation with respect to the interaction. The precise definition of the regime where effects arising from the particle interactions dominate is $\omega \leq C < \infty$ as g (and perhaps Ω) tend to infinity. We note that for $g \to \infty$ both $\underline{\varepsilon}$ and $\bar{\varepsilon}$ tend to zero. This is the main reason for the need of the different scalings, because the vanishing prefactors in the kinetic term allow the derivation of an upper bound on the energy.

The case of a dominating rotational energy contribution is then described as $\omega \to \infty$ as both $\Omega, g \to \infty$. Hence we need yet another scaling, which turns out as more convenient in the treatment of the associated TF functional (see section 4.5). Starting with (3.10) and choosing

$$\lambda \equiv \Omega^{2/(s-2)} \tag{3.18}$$

sets the term $\Omega^2 \lambda^{2-s}$ to one and yields

$$\begin{aligned}\mathcal{E}^{\mathrm{GP}}_{g,\Omega}[\phi] &= \underline{\Omega}^{-4/(s+2)} \int_{\mathbb{R}^3} \mathrm{d}\vec{x}' \left\{ \left| \left(\vec{\nabla}_{\vec{r}'} + \underline{\Omega}^{-\alpha} \vec{\nabla}_{z'} - i\vec{A}_{\underline{\Omega}} \right) \phi' \right|^2 \right. \\ &\qquad \left. + \underline{\Omega}^2 \left(\left(r'^s + |z'|^t \right) |\phi'|^2 - \tfrac{1}{4} r'^2 |\phi'|^2 + \gamma |\phi'|^4 \right) \right\} \\ &\equiv \underline{\Omega}^{-4/(s+2)} \mathcal{E}^{\mathrm{GP}}_{\gamma,\underline{\Omega}}[\phi'] \end{aligned} \tag{3.19}$$

with

$$\underline{\Omega}^2 \equiv \Omega^{2(s+2)/(s-2)} \tag{3.20}$$

and

$$\gamma \equiv g \Omega^{-2(s+(s+2)t)/((s-2)t)}. \tag{3.21}$$

For $s < t$ we take (3.10) and apply

$$\mu \equiv \Omega^{2s/((s-2)t)} \tag{3.22}$$

to get

$$\begin{aligned}\mathcal{E}^{\mathrm{GP}}_{g,\Omega}[\phi] &= \bar{\Omega}^{-4/(t+2)} \int_{\mathbb{R}^3} \mathrm{d}\vec{x}' \left\{ \left| \left(\bar{\Omega}^{-\beta} \vec{\nabla}_{\vec{r}'} + \vec{\nabla}_{z'} - i\vec{A}_{\bar{\Omega}} \right) \phi' \right|^2 \right. \\ &\qquad \left. + \bar{\Omega}^2 \left(\left(r'^s + |z'|^t \right) |\phi'|^2 - \tfrac{1}{4} r'^2 |\phi'|^2 + \gamma |\phi'|^4 \right) \right\} \\ &\equiv \bar{\Omega}^{-4/(t+2)} \dot{\mathcal{E}}^{\mathrm{GP}}_{\gamma,\bar{\Omega}}[\phi'] \end{aligned} \tag{3.23}$$

where

$$\bar{\Omega}^2 \equiv \Omega^{2s(t+2)/((s-2)t)} \tag{3.24}$$

and γ as in (3.21). The limit $\omega \to \infty$ is thus equivalent to $\gamma \to 0$ due to the relation

$$\gamma = \omega^{-(s-2)t/(s+(s+2)t)}. \tag{3.25}$$

Note that the prefactors $\underline{\Omega}^{-\alpha}$ and $\bar{\Omega}^{-\beta}$ in the kinetic term vanishing as $\Omega \to \infty$.

4 The Thomas-Fermi (TF) Framework

We will show that in the limit of $g \to \infty$ the magnetic-kinetic term of the GP functional (3.8) will become negligible and the situation can be described in terms of the *TF functional*

$$\mathcal{E}^{\mathrm{TF}}_{g,\Omega}[\rho] \equiv \int_{\mathbb{R}^3} \mathrm{d}\vec{x} \left\{ \left(r^s + |z|^t \right) \rho - \tfrac{1}{4}\Omega^2 r^2 \rho + g\rho^2 \right\} \tag{4.1}$$

defined on the domain

$$\mathcal{D}^{\mathrm{TF}} \equiv \left\{ \rho \in L^2\left(\mathbb{R}^3\right) \middle| \rho \geq 0, \left(r^s + |z|^t \right) \rho \in L^1\left(\mathbb{R}^3\right) \right\}. \tag{4.2}$$

4.1 Scaling of the TF Functional

By the same scalings that were used for the GP functionals (see (3.9)-(3.11)) we get matching expressions for the TF functionals. An essential property of these scalings is the fact that they reduce the TF problem to a one-parameter theory as the dependence of both Ω and g is combined into either ω or γ.

Using the independent scalings of $\vec{r}$ and z we obtain the relation

$$\mathcal{E}^{\mathrm{TF}}_{g,\Omega}[\rho] = \int_{\mathbb{R}^3} \mathrm{d}\vec{x}' \left\{ \left(\lambda^s r'^s + \mu^t |z'|^t \right) \rho' - \tfrac{1}{4}\Omega^2 \lambda^2 r'^2 \rho' + g\lambda^{-2}\mu^{-1}\rho'^2 \right\}$$

with $\rho(r,z) = \lambda^{-2}\mu^{-1}\rho'(r',z')$. For a dominating interaction energy contribution to the total energy we set the parameters λ and μ as in (3.12) and get the scaled TF functional

$$\begin{aligned} \mathcal{E}^{\mathrm{TF}}_{g,\Omega}[\rho] &= g^{st/(s+(s+2)t)} \int_{\mathbb{R}^3} \mathrm{d}\vec{x}' \left\{ \left(r'^s + |z'|^t \right) \rho' - \tfrac{1}{4}\omega r'^2 \rho' + \rho'^2 \right\} \\ &\equiv \varepsilon^{-2s/(s+2)} \mathcal{E}^{\mathrm{TF}}_{1,\omega}[\rho']. \end{aligned}$$

The corresponding *TF energy* is defined as the functional's infimum over all functions in $\mathcal{D}^{\mathrm{TF}}$, i.e.,

$$E^{\mathrm{TF}}_{1,\omega} \equiv \inf_{\rho \in \mathcal{D}^{\mathrm{TF}}, \|\rho\|_1 = 1} \mathcal{E}^{\mathrm{TF}}_{1,\omega}[\rho]. \tag{4.3}$$

It is known that this minimization problem has a unique solution, the *TF density*, given by

$$\rho^{\mathrm{TF}}_{1,\omega}(\vec{x}) = \frac{1}{2} \left[\mu^{\mathrm{TF}}_{1,\omega} + \tfrac{1}{4}\omega^2 r^2 - r^s - |z|^t \right]_+ \tag{4.4}$$

where $[\cdot]_+$ denotes the positive part and $\mu^{\mathrm{TF}}_{1,\omega}$ is the *TF chemical potential* fixed by the normalization $\|\rho^{\mathrm{TF}}_{1,\omega}\|_1 = 1$.

The relation

$$\mu^{\mathrm{TF}}_{1,\omega} = E^{\mathrm{TF}}_{1,\omega} + \|\rho^{\mathrm{TF}}_{1,\omega}\|_2^2 \tag{4.5}$$

can be obtained by multiplying (4.4) by $\rho^{\mathrm{TF}}_{1,\omega}$ and integrating the expression. The relationship between the scaled entities and the original ones is given by

$$\varepsilon^{2s/(s+2)} E^{\mathrm{TF}}_{g,\Omega} = E^{\mathrm{TF}}_{1,\omega} \qquad \text{and} \qquad \varepsilon^{2s/(s+2)} \mu^{\mathrm{TF}}_{g,\Omega} = \mu^{\mathrm{TF}}_{1,\omega}.$$

The TF density scales with

$$\varepsilon^{-2(s+2t)/((s+2)t)} \rho^{\mathrm{TF}}_{g,\Omega}\left(\varepsilon^{-2/(s+2)}\vec{r}, \varepsilon^{-2s/((s+2)t)} z \right) = \rho^{\mathrm{TF}}_{1,\omega}(\vec{r}, z). \tag{4.6}$$

If the rotational energy contribution is dominant, we use a different scaling akin to (3.18) and (3.22) to arrive at

$$\begin{aligned}\mathcal{E}^{\mathrm{TF}}_{g,\Omega}[\rho] &= \Omega^{2s/(s-2)} \int_{\mathbb{R}^3} \mathrm{d}\vec{x}' \left\{ \left(r'^s + |z'|^t \right) \rho' - \tfrac{1}{4} r'^2 \rho' + \gamma \rho'^2 \right\} \\ &\equiv \underline{\Omega}^{2s/(s+2)} \mathcal{E}^{\mathrm{TF}}_{\gamma,1}[\rho'].\end{aligned} \tag{4.7}$$

The corresponding TF density is given by

$$\rho^{\mathrm{TF}}_{\gamma,1}(\vec{x}) = \frac{1}{2\gamma} \left[\mu^{\mathrm{TF}}_{\gamma,1} + \tfrac{1}{4} r^2 - r^s - |z|^t \right]_+ \tag{4.8}$$

and its energy, defined as in (4.3), exhibits the relation

$$\mu^{\mathrm{TF}}_{\gamma,1} = E^{\mathrm{TF}}_{\gamma,1} + \gamma \|\rho^{\mathrm{TF}}_{\gamma,1}\|_2^2$$

with $\mu^{\mathrm{TF}}_{\gamma,1}$ fixed again by normalization of the density. The scalings of these quantities are given by

$$\underline{\Omega}^{-2s/(s+2)} E^{\mathrm{TF}}_{g,\Omega} = E^{\mathrm{TF}}_{\gamma,1},\ \underline{\Omega}^{-2s/(s+2)} \mu^{\mathrm{TF}}_{g,\Omega} = \mu^{\mathrm{TF}}_{\gamma,1}$$

and

$$\underline{\Omega}^{2(s+2t)/((s+2)t)} \rho^{\mathrm{TF}}_{g,\Omega} \left(\underline{\Omega}^{-2/(s+2)} \vec{r}, \underline{\Omega}^{-2s/((s+2)t)} z \right) = \rho^{\mathrm{TF}}_{\gamma,1}(\vec{r}, z).$$

The energies we defined in this section so far will give the leading order term of the GP energy as g and possibly Ω tend to infinity. To further illustrate this framework we derive additional properties of the TF density and show plots of the density with different parameter choices.

4.2 The Support of the TF Densities

To simplify the notation throughout this section we will write ρ^{TF} whenever a statement holds for both $\rho^{\mathrm{TF}}_{1,\omega}$ and $\rho^{\mathrm{TF}}_{\gamma,1}$. Furthermore we denote with the constant c_1 either ω^2 or 1, whichever is appropriate for the choice of the density in the same context. The same holds for c_2, which is either 1 or γ. Both constants are positive since Ω and g are positive. The TF densities given by (4.4) and (4.8) are rotationally symmetric and we can abbreviate with $\rho^{\mathrm{TF}}(r, z)$ the expression $\rho^{\mathrm{TF}}(r, \phi, z)$ for an arbitrarily but fixed angular component ϕ of the cylindrical coordinates.

Since $s > 2$ and $t > 0$ the expressions $\left(\frac{1}{4} c_1 r^2 - r^s\right)$ and $\left(-|z|^t\right)$ tend to $-\infty$ for $r \to \infty$ and $z \to \pm\infty$. This ensures that ρ^{TF} is compactly supported[4], i.e. $\mathrm{supp}(\rho^{\mathrm{TF}}) \subset \mathcal{B}_R$ for some $R < \infty$ depending on ω or γ.

For our further investigations of the support we define the function

$$f(y, w) \equiv \frac{1}{2c_2} \left(\mu^{\mathrm{TF}} + \tfrac{1}{4} c_1 y - y^{s/2} - w^2 \right) \tag{4.9}$$

using cylindrical coordinates. Choosing the respective values for the constants c_1 and c_2 one can easily see that $\rho^{\mathrm{TF}} = \left[f(r^2, |z|^{t/2}) \right]_+$.

Taking the second partial derivatives of f with respect to y and w we see that

$$\frac{\partial^2 f}{\partial y^2} = -\frac{s(s-2)}{8c_2} y^{(s-4)/2} < 0, \quad \text{for } y \geq 0 \tag{4.10}$$

[4] $\mathcal{B}_R$ denotes a three-dimensional ball centered at the origin with radius R.

and

$$\frac{\partial^2 f}{\partial w^2} = -\frac{1}{c_2} < 0 \quad \text{for } w \in \mathbb{R}. \tag{4.11}$$

This implies that f is strictly concave along radial rays[5] (that are perpendicular to the w-axis) and along lines parallel to the w-axis.

If we assume that f is positive at a point $\vec{x}_0$, then concavity ensures that along a line, parallel to the w-axis that contains $\vec{x}_0$, the function f vanishes at two points. Due to the symmetry of f in w these two points' w-coordinates differ only by sign. The same procedure with respect to a radial ray yields that, depending on the value of f at $y = 0$, f has one or two zeros along the ray. In the case of $f \leq 0$ at the w-axis it vanishes at two points and in the case of a strictly positive value it has only one zero. By construction f is radially symmetric and with the results above this implies that the support of f is connected since f (as well as ρ^{TF}) are continuous. Note that $\rho^{\mathrm{TF}}(r,0) = \max_{z' \in \mathbb{R}} \rho^{\mathrm{TF}}(r,z')$ because $\partial\rho^{\mathrm{TF}}/\partial z = -\frac{1}{2}t\,|z|^{t-1} < 0$ for $z \neq 0$. In the origin we have $f(0) = \mu^{\mathrm{TF}}/(2c_2)$ and thus the number of zeros along a ray in the $z = 0$ plane is governed by the sign of μ^{TF}.

If $\mu^{\mathrm{TF}} > 0$, then there exists a unique $y_{\mathrm{out}} > 0$ such that $f(y_{\mathrm{out}}, 0) = 0$. By the definition of f we see that the support of ρ^{TF} along such a ray is the interval $[0, R_{\mathrm{out}}]$, with $R_{\mathrm{out}} \equiv \sqrt{y_{\mathrm{out}}}$. To abbreviate the notation we define the $\{z = 0\}$-plane as

$$\mathcal{P} = \left\{(r,z) \in \mathbb{R}^3 | z = 0\right\}. \tag{4.12}$$

By the radial symmetry of the TF density we see that the support in $\mathcal{P}$ is, in fact, a disc with radius R_{out} centered at the origin.

In the case of $\mu^{\mathrm{TF}} < 0$ there exist two distinct radii y_{in} and y_{out} such that $f(y_{\mathrm{in}}, 0) = f(y_{\mathrm{out}}, 0) = 0$. Hence the support of ρ^{TF} in $\mathcal{P}$ is a ring with inner radius R_{in} and outer radius R_{out}, where R_{out} is defined as above and $R_{\mathrm{in}} \equiv \sqrt{y_{\mathrm{in}}}$.

Since the density vanishes at these points we have that $\mu^{\mathrm{TF}} = R_{\mathrm{out}}^s - \frac{1}{4}c_1 R_{\mathrm{out}}^2$ and, in the case of $\mu^{\mathrm{TF}} < 0$, $\mu^{\mathrm{TF}} = R_{\mathrm{in}}^s - \frac{1}{4}c_1 R_{\mathrm{in}}^2$. If $\mu^{\mathrm{TF}} = 0$, the density is zero in the origin and the support of ρ^{TF} intersected with $\mathcal{P}$ is the disc with radius R_{out}.

Having established a rough description of the density's support in $\mathcal{P}$, we have to examine its properties in the z-direction. We start by defining the circle of maximum density by $\{(R_{\max}, \phi, 0) | 0 \leq \phi < 2\pi\}$ with

$$R_{\max} \equiv \left(\frac{c_1}{2s}\right)^{1/(s-2)} \tag{4.13}$$

justified by $\partial\rho^{\mathrm{TF}}/\partial r = 0$ at $r = R_{\max}$. The density's decrease in z-direction is independent of r and therefore it has its largest elongation $2Z_{\mathrm{out}}$ (parallel to the rotational axis) at radial coordinate $R_{\max}$ with

$$Z_{\mathrm{out}} \equiv \left(\mu^{\mathrm{TF}} + 4^{1/(s-2)}(s-2)\left(\frac{c_1}{4s}\right)^{s/(s-2)}\right)^{1/t}. \tag{4.14}$$

Let $\zeta(r)$ be the function that assigns every radius ($\max\{0, R_{\mathrm{in}}\} \leq r \leq R_{\mathrm{out}}$) the smallest modulus of the z-coordinate at which the density vanishes, i.e., $\zeta(r) \equiv \inf_{z \in \mathbb{R}} \left\{|z| \,|\, \rho^{\mathrm{TF}}(r,z) = 0\right\}$. Since the density is strictly positive on $\{(r,\phi,0) \,|\, r \in (R_{\mathrm{in}}, R_{\mathrm{out}}) \wedge \phi \in [0, 2\pi)\}$, the same holds for ζ by continuity of ρ^{TF}. On the support of the TF density we can solve $f(r^2, \zeta(r)^{t/2}) = 0$ explicitly and get

$$\zeta(r) = \left(\mu^{\mathrm{TF}} + \tfrac{1}{4}c_1 r^2 - r^s\right)^{1/t}. \tag{4.15}$$

Not surprisingly we have $\zeta(R_{\max}) = Z_{\mathrm{out}}$ and $\partial\zeta/\partial r = 0$ at $r = R_{\max}$.

[5] A radial ray is a set $\left\{(r,\phi,z) \in \mathbb{R}^3 | r \geq 0, \phi \text{ const.}, z \text{ const.}\right\}$ in cylindrical coordinates.

4.3 The Behavior of the Support near $z = 0$

By looking at the derivative of ζ we can derive statements about the smoothness of the density's envelope, i.e. the border of its support, close to $\mathcal{P}$. Evaluating

$$\zeta'(r) = \frac{1}{t}\left(\mu^{\mathrm{TF}} + \tfrac{1}{4}c_1 r^2 - r^s\right)^{(t-1)/t}\left(\tfrac{1}{2}c_1 r - s r^{s-1}\right) \quad c_1 \text{ as above} \tag{4.16}$$

shows that this behavior depends on the value of the exponent $(t-1)/t$. Since the term under this exponent vanishes at R_{out} and, if $\mu^{\mathrm{TF}} \leq 0$, at R_{in}, one has three different limits listed below. Note that interesting properties arise for $t \leq 1$ due to the non-differentiability of the external potential at $z = 0$. Since the main results in Section 5 are proved even for this case we will need a clear picture of the possible complications we will face.

- $\mathbf{0 < t < 1}$
  implies that the exponent $(t-1)/t$ is positive and $\zeta'(r) \to 0$ as $r \to R_{\mathrm{out}}$. If $\mu^{\mathrm{TF}} \geq 0$ we also have that $\zeta'(r) \to 0$ as $r \to 0$ whereas, if $\mu^{\mathrm{TF}} < 0$ we see that $\zeta'(r) \to 0$ as $r \to R_{\mathrm{in}}$. Thus the envelope has infinitely sharp edges at the circles with radii R_{out} and (possibly) R_{in} where it intersects $\mathcal{P}$ (see figure 1). From $\mu^{\mathrm{TF}} > 0$ follows $\zeta(0) > 0$ and the envelope has a local minimum around the origin (since $\zeta''(0) = c_1 {\mu^{\mathrm{TF}}}^{(t-1)/t}/(2t) > 0$).

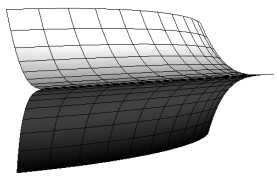

Fig. 1: infinitely sharp edge

- $\mathbf{t > 1}$
  gives a negative exponent and $\zeta'(r) \to -\infty$ as $r \to R_{\mathrm{out}}$, showing that the envelope of the density intersect $\mathcal{P}$ perpendicularly (see figure 2).

  The sign is due to the term $\left(\frac{1}{2}c_1 r - s r^{s-1}\right)$ which is negative at $r = R_{\mathrm{out}}$. We easily see that by realizing that its roots are at $r = 0$ and $r = R_{\mathrm{max}}$. Furthermore it tends to $-\infty$ as $r \to \infty$ and we have that $0 < R_{\mathrm{max}} < R_{\mathrm{out}}$.

  If $\mu^{\mathrm{TF}} > 0$ we get that $\zeta'(r) \to 0$ as $r \to 0$ and, as in the case above, the envelope has a local minimum around $r = 0$. For $\mu^{\mathrm{TF}} = 0$ the same holds by l'Hôspital's rule. If $\mu^{\mathrm{TF}} < 0$ we have an inner radius at which the first derivative diverges and we get, as above for R_{out}, that the density's envelope and $\mathcal{P}$ meet at a normal angle, i.e., $\zeta'(r) \to \infty$ as $r \to R_{\mathrm{in}}$ since $0 < R_{\mathrm{in}} < R_{\mathrm{max}}$.

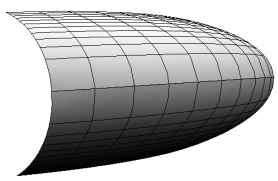

Fig. 2: orthogonal intersection

- $\boldsymbol{t = 1}$
  zeros the exponent and the derivative simplifies to

$$\zeta_1{}'(r) = \left(\tfrac{1}{2}c_1 r - s r^{s-1}\right)/t. \tag{4.17}$$

At R_{out} it takes a finite strictly negative value, which can be pictured as the density's envelope having a sharp (but not infinitely sharp) edge where it intersects $\mathcal{P}$ (see figure 3). If $\mu^{\text{TF}} < 0$ the same holds at R_{in} (but with opposite sign).

For $\mu^{\text{TF}} = 0$ we have the infinitely sharp edge at the origin and $\mu^{\text{TF}} > 0$ the density's envelope has again a minimum at the $r = 0$.

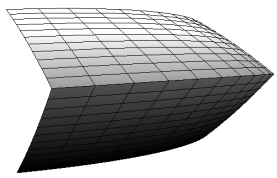

Fig. 3: sharp edge

4.4 Explicit Calculations of the TF Densities

To get an explicit expression of the TF density one has to calculate the exact dependency of μ^{TF} on g and Ω. While such formulas are in general not available it is nevertheless possible to obtain them in two important special cases.

4.4.1 The Non-Rotational Case, $\Omega = 0$

For this case we use the scaled density $\rho^{\text{TF}}_{1,\omega}$ since $\Omega = 0$ implies $1/\gamma = \infty$. In the following we calculate the full dependency of $\mu^{\text{TF}}_{1,0}$ on s and t.

To achieve this we use the normalization condition $\|\rho^{\text{TF}}_{1,0}\|_1 = 1$ after we have determined the domain of integration. By (4.13) it is clear that $\mu^{\text{TF}}_{1,0} > 0$ and by section 4.2 we know that our support in $\mathcal{P}$ is a disc with radius $r^+ = (\mu^{\text{TF}}_{1,0})^{1/s}$. In z-direction we get the upper and lower limit by $\rho^{\text{TF}}_{1,0}(r, z^\pm) = 0$, yielding $z^\pm = \pm\left(\mu^{\text{TF}}_{1,0} - r^s\right)^{1/t}$. The normalization condition gives

$$1 = \frac{1}{2}\int_0^{2\pi}\int_0^{r^+}\int_{z^-}^{z^+}\left(\mu^{\text{TF}}_{1,0} - r^s - |z|^t\right) r\mathrm{d}z\,\mathrm{d}r\,\mathrm{d}\phi$$

and by symmetry in z-direction

$$\begin{aligned}
&= 2\pi\int_0^{r^+}\int_0^{z^+}\left(\mu^{\text{TF}}_{1,0} - r^s - |z|^t\right) r\mathrm{d}z\,\mathrm{d}r \\
&= \frac{2\pi t}{t+1}\int_0^{r^+}\left(\mu^{\text{TF}}_{1,0} - r^s\right)^{1+1/t} r\mathrm{d}r \\
&= \frac{2\pi t}{s(t+1)}\,\mathrm{B}\left(\frac{2}{s}, 2 + \frac{1}{t}\right)\mu^{\text{TF}}_{1,0}{}^{1+2/s+1/t} \\
&= \frac{2\pi}{s}\frac{\Gamma\left(\frac{2}{s}\right)\Gamma\left(1+\frac{1}{t}\right)}{\Gamma\left(2+\frac{2}{s}+\frac{1}{t}\right)}\mu^{\text{TF}}_{1,0}{}^{(s+(s+2)t)/(st)}.
\end{aligned}$$

where $\mathrm{B}(\cdot,\cdot)$ is the Beta function and $\Gamma(\cdot)$ the Gamma function. By solving the equality we get

$$\mu^{\text{TF}}_{1,0} = \left(\frac{2\pi t}{s(t+1)}\,\mathrm{B}\left(\frac{2}{s}, 2 + \frac{1}{t}\right)\right)^{-st/(s+(s+2)t)} \tag{4.18}$$

and thus the full description of $\rho^{\text{TF}}_{1,0}$.

4.4.2 The Emergence of a 'hole', $\mu_{1,\omega}^{\mathrm{TF}} = 0$

Another special case for which the full evaluation can be obtained is for $\mu_{1,\omega}^{\mathrm{TF}} = 0$. As seen in section 4.2 this is the smallest value of the chemical potential such that the support of the density intersected with $\mathcal{P}$ does not have a hole around the origin. This allows us to calculate the relationship ω_0 between g and Ω such that $\mu_{1,\omega_0}^{\mathrm{TF}} = 0$. As in the section above we easily obtain the limits as $r^+ = (\omega_0/2)^{1/(s-2)}$ and $z^\pm = \pm(\frac{1}{4}{\omega_0}^2 r^2 - r^s)^{1/t}$ and we get

$$1 = \frac{1}{2}\int_0^{2\pi}\int_0^{r^+}\int_{z^-}^{z^+}\left(\tfrac{1}{4}{\omega_0}^2 r^2 - r^s - |z|^t\right) r\mathrm{d}z\,\mathrm{d}r\,\mathrm{d}\phi$$

and by symmetry in z-direction

$$\begin{aligned}
&= 2\pi\int_0^{r^+}\int_0^{z^+}\left(\tfrac{1}{4}{\omega_0}^2 r^2 - r^s - |z|^t\right) r\mathrm{d}z\,\mathrm{d}r \\
&= \frac{2\pi t}{t+1}\int_0^{r^+}\left(\tfrac{1}{4}{\omega_0}^2 r^2 - r^s\right)^{1+1/t} r\mathrm{d}r \\
&= \frac{2\pi t}{(s-2)(t+1)}\,\mathrm{B}\left(\frac{2(2t+1)}{(s-2)t}, 2+\frac{1}{t}\right)\left(\frac{\omega_0}{2}\right)^{2(s+(s+2)t)/((s-2)t)}.
\end{aligned}$$

By solving the equation we get the precise value of ω_0, namely,

$$\omega_0 = 2\left(\frac{2\pi t}{(s-2)(t+1)}\,\mathrm{B}\left(\frac{2(2t+1)}{(s-2)t}, 2+\frac{1}{t}\right)\right)^{-(s-2)t/(2(s+(s+2)t))}. \tag{4.19}$$

The relation (3.25) determines the value γ_0 such that $\mu_{\gamma_0,1}^{\mathrm{TF}} = 0$, i.e.,

$$\gamma_0 = 2^{-2(s+(s+2)t)/((s-2)t)}\frac{2\pi t}{(s-2)(t+1)}\,\mathrm{B}\left(\frac{2(2t+1)}{(s-2)t}, 2+\frac{1}{t}\right). \tag{4.20}$$

4.4.3 The General Case

For arbitrary values of ω an explicit calculation is not possible and we will briefly show the arising problems. For $\rho_{1,\omega}^{\mathrm{TF}}$ and $\rho_{\gamma,1}^{\mathrm{TF}}$ we can still derive the lower and upper integration limits in z, namely, $z^\pm = \pm(\mu_{1,\omega}^{\mathrm{TF}} + \frac{1}{4}\omega^2 r^2 - r^s)^{1/t}$ (resp. $z^\pm = \pm(\mu_{\gamma,1}^{\mathrm{TF}} + \frac{1}{4}r^2 - r^s)^{1/t}$) but the equations determining the limits in r are not explicitly solvable in general, i.e.,

$$\mu_{1,\omega}^{\mathrm{TF}} + \tfrac{1}{4}\omega^2 r^{\pm 2} - r^{\pm s} = 0 \quad \text{resp.} \quad \mu_{\gamma,1}^{\mathrm{TF}} + \tfrac{1}{4}r^{\pm 2} - r^{\pm s} = 0$$

due to the possibilities of $s \notin \{3,4,6,8\}$, $\omega > 0$, $\mu_{1,\omega}^{\mathrm{TF}} \neq 0$ or $\mu_{\gamma,1}^{\mathrm{TF}} \neq 0$.

Evaluating the integrations in ϕ and z yields

$$\begin{aligned}
1 &= \frac{1}{2}\int_0^{2\pi}\int_{r^-}^{r^+}\int_{z^-}^{z^+}\left(\mu_{1,\omega}^{\mathrm{TF}} + \tfrac{1}{4}\omega^2 r^2 - r^s - |z|^t\right) r\mathrm{d}z\,\mathrm{d}r\,\mathrm{d}\phi \\
&= \frac{2\pi t}{t+1}\int_{r^-}^{r^+}\left(\mu_{1,\omega}^{\mathrm{TF}} + \tfrac{1}{4}\omega^2 r^2 - r^s\right)^{1+1/t} r\mathrm{d}r
\end{aligned}$$

resp.

$$\begin{aligned}
1 &= \frac{1}{2\gamma}\int_0^{2\pi}\int_{r^-}^{r^+}\int_{z^-}^{z^+}\left(\mu_{\gamma,1}^{\mathrm{TF}} + \tfrac{1}{4}r^2 - r^s - |z|^t\right) r\mathrm{d}z\,\mathrm{d}r\,\mathrm{d}\phi \\
&= \frac{2\pi t}{\gamma(t+1)}\int_{r^-}^{r^+}\left(\mu_{\gamma,1}^{\mathrm{TF}} + \tfrac{1}{4}r^2 - r^s\right)^{1+1/t} r\mathrm{d}r\,,
\end{aligned}$$

whereas it is not generally possible to explicitly calculate the remaining integration in r.

4.5 Limit of the TF Density as $\omega \to \infty$ ($\gamma \to 0$)

In the case of a dominating rotational energy contribution to the total energy the parameter ω diverges as Ω and g tend to infinity. To clarify this behavior we will derive the asymptotics for both the density's support and the corresponding TF energy. This will show a convergence of the support to a circle in the $\{z = 0\}$ plane and a convergence of the energy to

$$E_{0,1}^{\mathrm{TF}} \equiv \min_{\vec{x}\in\mathbb{R}^3} \left\{ r^s + |z|^t - \tfrac{1}{4}r^2 \right\} < 0 \quad \text{as } \gamma \to 0.$$

This behavior is illustrated by the plots in Fig. 16-21 in section 4.6.

Lemma 4.1 (Support of the TF density as $\omega \to \infty$) *For $\gamma \to 0$ the density $\rho_{\gamma,1}^{\mathrm{TF}}$ becomes concentrated around a circle in $\mathcal{P}$ centered at the origin with radius $(2s)^{-1/(s-2)}$. More precisely, for decreasing γ the density vanishes at every point with strictly positive distance from this circle.*

Proof: By normalization of the TF density we have that

$$1 = \left\|\rho_{\gamma,1}^{\mathrm{TF}}\right\|_1 = \frac{1}{2\gamma}\int_{\mathbb{R}^3} \mathrm{d}\vec{x}\, \left[\mu_{\gamma,1}^{\mathrm{TF}} - r^s - |z|^t + \tfrac{1}{4}r^2\right]_+$$

and see that the integrand has to vanish with decreasing γ. This, and the fact that the density has to be positive somewhere, demand that $\mu_{\gamma,1}^{\mathrm{TF}} \to E_{0,1}^{\mathrm{TF}}$ from above as $\gamma \to 0$. The set where the density attains its maximum is given by

$$\left\{(\vec{r}, z) \in \mathbb{R}^3 \,\middle|\, -r^s - |z|^t + \tfrac{1}{4}r^2 = -E_{0,1}^{\mathrm{TF}} \right\} = \left\{(\vec{r}, z) \in \mathbb{R}^3 \,\middle|\, r = (2s)^{-1/(s-2)} \wedge z = 0 \right\} \tag{4.21}$$

and is the circle described in the lemma above. By simple substitution we obtain the limit of the chemical potential, namely,

$$\mu_{\gamma,1}^{\mathrm{TF}} \xrightarrow{\gamma\to 0} (2s)^{-s/(s-2)} - \tfrac{1}{4}(2s)^{-2/(s-2)} \equiv \mu_{0,1}^{\mathrm{TF}} \left(= E_{0,1}^{\mathrm{TF}}\right).$$

If we take a point $\vec{x}' = (\vec{r}\,', z')$ with strictly positive distance from this circle, we see that

$$\left(\mu_{\gamma,1}^{\mathrm{TF}} - r'^s - |z'|^t + \tfrac{1}{4}r'^2\right) \xrightarrow{\gamma\to 0} \left(\mu_{0,1}^{\mathrm{TF}} - r'^s - |z'|^t + \tfrac{1}{4}r'^2\right) < \mu_{0,1}^{\mathrm{TF}} - E_{0,1}^{\mathrm{TF}} = 0$$

and the density vanishes for γ small enough (due to the function $[\,\cdot\,]_+$).

□

We can use this result to derive the asymptotics of the TF energy.

Lemma 4.2 (TF energy as $\omega \to \infty$) *For $\gamma \to 0$ we have*

$$E_{\gamma,1}^{\mathrm{TF}} = E_{0,1}^{\mathrm{TF}} + \begin{cases} O\left(\gamma^{1/2}\right) & \text{if } t \geq 2 \\ O\left(\gamma^{t/(t+2)}\right) & \text{if } t \leq 2 \end{cases} \tag{4.22}$$

Proof: Inspired by lemma 4.1 we will evaluate the TF functional on a radially symmetric trial function, the support of which becomes concentrated around a circle. Let $f(x,y)$ be a continuous, nonnegative function with support in the unit disc $\mathcal{D}$ around the origin in $\mathbb{R}^2$. Furthermore we demand that $\iint f(x,y)\,\mathrm{d}x\,\mathrm{d}y = (2\pi r_0)^{-1}$ and $\iint f(x,y)\,x\,\mathrm{d}x\,\mathrm{d}y = 0$ where $r_0 \equiv (2s)^{-1/(s-2)}$. Our trial function defined in cylindrical coordinates is

$$\tilde{\rho}_\tau(r,\phi,z) \equiv \tau^{-2} f\left(\frac{r-r_0}{\tau}, \frac{z}{\tau}\right) \quad \text{for } \ 0<\tau<r_0. \tag{4.23}$$

We immediately see the support of $\tilde{\rho}_\tau$ lies in a torus with main radius r_0 and inner radius τ. The circle that lies at the center of the torus' tube is the same circle as in (4.21). The additional demands on f ensure that $\int \tilde{\rho}_\tau = 1$ for all $0<\tau<r_0$. We are interested in the value of the TF functional (4.7) evaluated on $\tilde{\rho}_\tau$ in the limit of $\tau \to 0$; in which the support of the trial function becomes concentrated around the circle described in lemma 4.1.

At first we consider the case $t \geq 2$. We see that $r^s + |z|^t - \frac{1}{4}r^2$ is twice differentiable and thus Taylor expansion around $r = r_0$ yields

$$\begin{aligned} E^{\mathrm{TF}}_{\gamma,1} \leq \mathcal{E}^{\mathrm{TF}}_{\gamma,1}[\tilde{\rho}_\tau] &= \int_{\mathbb{R}^3} \mathrm{d}\vec{x}\, \left\{ \left(r^s + |z|^t - \tfrac{1}{4}r^2\right)\tilde{\rho}_\tau + \gamma\tilde{\rho}_\tau^2 \right\} \\ &\leq E^{\mathrm{TF}}_{0,1} + C\tau^2 + \gamma\tau^{-2}2\pi r_0 \|f\|_2^2 \end{aligned}$$

and, by choosing $\tau = \gamma^{1/4}$,

$$\leq E^{\mathrm{TF}}_{0,1} + C\gamma^{1/2}.$$

In the case of $t \leq 2$ we have that

$$\begin{aligned} E^{\mathrm{TF}}_{\gamma,1} &\leq E^{\mathrm{TF}}_{0,1} + C\tau^t + \gamma\tau^{-2}2\pi r_0\|f\|_2^2 \\ &\leq E^{\mathrm{TF}}_{0,1} + C\gamma^{t/(t+2)} \end{aligned}$$

where we chose $\tau = \gamma^{1/(t+2)}$. The lower bound $E^{\mathrm{TF}}_{\gamma,1} \geq E^{\mathrm{TF}}_{0,1}$ comes from the trivial fact that $\mathcal{E}^{\mathrm{TF}}_{\gamma,0}[\rho] \leq \mathcal{E}^{\mathrm{TF}}_{\gamma,1}[\rho]$ for every function ρ (see (4.1)).

With a simpler trial function that has different growth rates in radial and z-direction it is possible to obtain a better bound. This function will not be used in further calculations however and therefore we give only a very short outline thereof. Using the function

$$\tilde{\rho}^s_\tau(r,z) \equiv \begin{cases} (8\pi r_0 \tau\nu)^{-1} & \text{if} \quad r_0 - \tau \leq r \leq r_0 + \tau \quad \wedge \quad -\nu \leq z \leq \nu \\ 0 & \text{otherwise,} \end{cases} \tag{4.24}$$

the support of which is a hollow cylinder, we can explicitly calculate $\mathcal{E}^{\mathrm{TF}}_{\gamma,1}[\tilde{\rho}^s_\tau]$. Setting $\tau \equiv \gamma^{t/(3t+2)}$ and $\nu \equiv \gamma^{2/(3t+2)}$ yields

$$E^{\mathrm{TF}}_{\gamma,1} = E^{\mathrm{TF}}_{0,1} + O\left(\gamma^{2t/(3t+2)}\right). \tag{4.25}$$

This is obviously a stronger bound but its underlying trial function proves unsuitable for subsequent calculations in Theorem 5.4.

□

4.6 Illustrations of the TF Density

To clarify the influence of s and t on the shape of the TF density (and therefore the asymptotic shape of the GP density) we show various plots of the TF density with different values of s, t, g and Ω. A gray-shade coded value of the density and the contour of its support will be depicted for radial slices.

The plots in this section were generated with the help of a self-developed *Mathematica* program. Its full source code can be found in appendix A.

Both $\rho^{\mathrm{TF}}_{g,\Omega}$ and $\rho^{\mathrm{TF}}_{1,\omega}$ are not suitable for the illustrations as the former's support diverges in all directions and the latter's support is scaled differently in radial and z-direction. As a compromise we use a uniformly scaled variant of $\rho^{\mathrm{TF}}_{g,\Omega}$, namely $\hat{\rho}$, which stays finite in the radial direction. Since the support of $\rho^{\mathrm{TF}}_{1,\omega}$ stays bounded for finite values of ω we use it as starting point for subsequent rescalings. By (4.6) it is clear which scaling of the radial direction has to be used. Denoting by $\vec{r}$ and z the *original coordinates* (which are used in (3.8)) we define the scaled coordinates as

$$\vec{r}\,' \equiv g^{-t/\sigma}\vec{r} \quad \text{and} \quad z' \equiv g^{-t/\sigma} z \tag{4.26}$$

where $\sigma \equiv s + (s+2)t$. This allows us to rewrite (4.6) as

$$g^{(s+2t)/\sigma}\rho^{\mathrm{TF}}_{g,\Omega}(\vec{r}, z) = \rho^{\mathrm{TF}}_{1,\omega}(\vec{r}\,', g^{-(s-t)/\sigma} z') \equiv g^{(s-t)/\sigma}\hat{\rho}(\vec{r}\,', z')$$

with $\hat{\rho}$ being a normalized function on $\mathbb{R}^3$.

Solving the equation

$$\rho^{\mathrm{TF}}_{1,\omega}(\vec{r}\,', g^{-(s-t)/\sigma} z') = 0$$

for z' we get, by using the explicit form of the scaled density (4.4),

$$|z'| \geq g^{(s-t)/\sigma}\left[\mu^{\mathrm{TF}}_{1,\omega} + \tfrac{1}{4}\omega^2 r'^2 - r'^s\right]_+^{1/t}. \tag{4.27}$$

From the calculations in section 4.2 we already know that for each radial distance r' the smallest value of $|z'|$ in (4.27) lies on the border of the density's support, as long as the point $(r', 0)$ lies in the support.

The prefactor $g^{(s-t)/\sigma}$ shows the main dependence of the border's shape on the external potential's parameters s and t. For $s > t$, the confinement of the density is stronger in radial direction and thus the density's support will grow more rapidly in z-direction as the rotational velocity is increased. Since we scaled the density to have a constant radial elongation we expect the support's border to grow in both positive and negative z-directions. This is indeed the case as $g^{(s-t)/\sigma} \to \infty$ as $g \to \infty$. In the converse case of $s < t$ the density's support grows faster in radial direction and thus we expect a shrinking in z-direction. This is again backed up by $g^{(s-t)/\sigma} \to 0$ as $g \to \infty$. For a completely homogeneous external potential, i.e. $s = t$, the shape of the scaled density's support does not change with g.

In the following pictures the smallest value of $|z'|$ that satisfy the inequality (4.27) will be represented by the thick black outline of the density whereas the actual value of $\hat{\rho}$ will be depicted as a gray scale. The following plots show a radial slice of the density $\hat{\rho}$ for the angles $\phi = 0$ and $\phi = \pi$ in the cylindrical coordinates.

With fixed values for s and t the value of the chemical potential $\mu^{\mathrm{TF}}_{1,\omega}$ decreases with increasing ω and we show the cases of it being larger than, equal to and smaller than zero.

For Fig. 4 to 6 we use $s = 4$, $t = 2$ and $g = 1$.

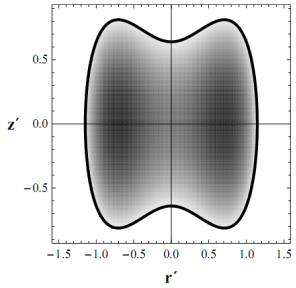

Fig. 4: $\omega = 2$, $\mu_{1,\omega}^{\mathrm{TF}} = 0.4104$

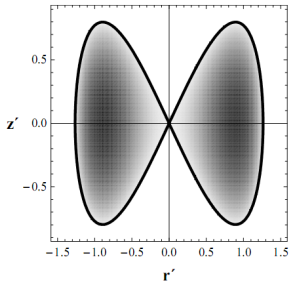

Fig. 5: $\omega = 2.5265$, $\mu_{1,\omega}^{\mathrm{TF}} = 0$

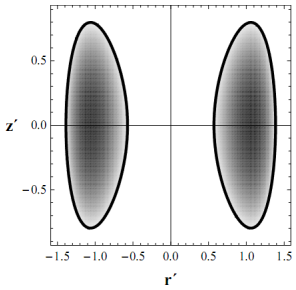

Fig. 6: $\omega = 3$, $\mu_{1,\omega}^{\mathrm{TF}} = -0.6290$

To illustrate the case of $s < t$ we choose $s = 4$, $t = 8$ and again $g = 1$. The same cases of $\mu_{1,\omega}^{\mathrm{TF}}$ as above are shown in Fig. 7 to 9 with similar values of ω .

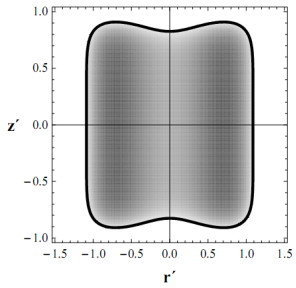

Fig. 7: $\omega = 2$, $\mu_{1,\omega}^{\mathrm{TF}} = 0.2174$

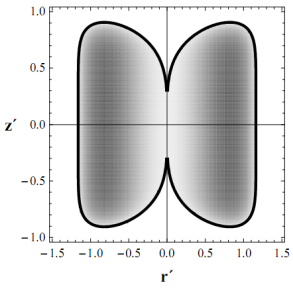

Fig. 8: $\omega = 2.3226$, $\mu_{1,\omega}^{\mathrm{TF}} = 0$

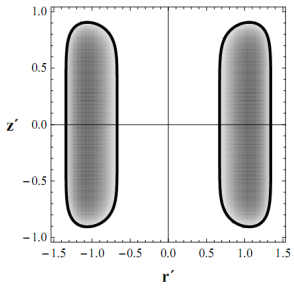

Fig. 9: $\omega = 3$, $\mu_{1,\omega}^{\mathrm{TF}} = -0.8109$

For all previous figures a white plot point indicates a vanishing density whereas the darkest shade of gray indicates the value $\hat{\rho} = 0.3302$ which stems from the largest value of the densities in all previous illustrations. The gray scale is then a linear interpolation between these two colors.

The next two sequences show the transformation of the density as g increases. For the case of $s > t$ we take the same values for ω and $\mu_{1,\omega}^{\mathrm{TF}}$ as in Fig. 4 but plot additional values of $g = 1, 10^2$ and 10^4 resulting in Fig. 10-12. Note that Fig. 10 is the same as Fig. 4 but with a different scale in the z-direction.

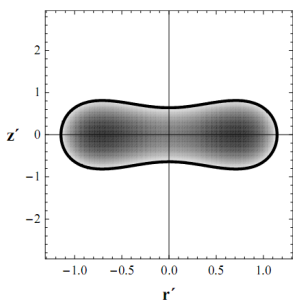

Fig. 10: $g = 1$

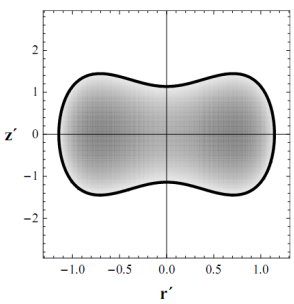

Fig. 11: $g = 10^2$

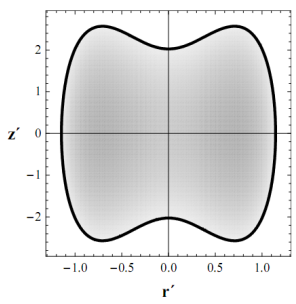

Fig. 12: $g = 10^4$

Again the highest depicted density of all three plots is $\hat{\rho} = 0.3302$.

The converse case of $s < t$ is shown by Fig. 13-15 with the same progression of g as above. Using Fig. 9 as the originating plot we can now observe the stronger confinement in z-direction.

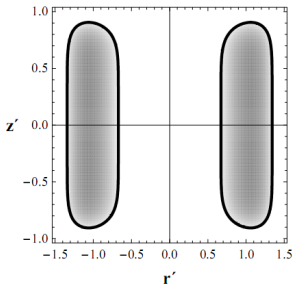

Fig. 13: $g = 1$

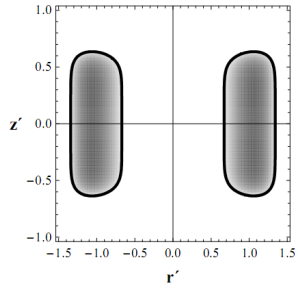

Fig. 14: $g = 10^2$

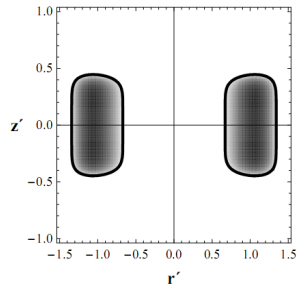

Fig. 15: $g = 10^4$

Due to the concentration of the density we use a different gray scale in the last three pictures with black indicating $\hat{\rho} = 0.4617$.

In the rest of this section we will show plots similar to the ones above but for the case of a diverging parameter ω. With the same intentions as in (4.26), i.e. to derive a suitable scaling of the density for our illustrations, we choose new coordinates

$$\vec{r}'' \equiv \Omega^{2/(s-2)}\vec{r} \quad \text{and} \quad z'' \equiv \Omega^{2/(s-2)} z$$

which we use for the definition of the normalized density $\check{\rho}$

$$\begin{aligned}\Omega^{2(s+2t)/((s-2)t)}\rho^{\mathrm{TF}}_{g,\Omega}(\vec{r}, z) &= \rho^{\mathrm{TF}}_{\gamma,1}(\vec{r}'', \Omega^{2(s-t)/((s-2)t)} z'') \\ &\equiv \Omega^{-2(s-t)/((s-2)t)}\check{\rho}(\vec{r}'', z''). \end{aligned} \tag{4.28}$$

We already know from lemma 4.1 that for decreasing γ the support of $\rho^{\mathrm{TF}}_{\gamma,1}$ becomes concentrated around a circle in $\mathcal{P}$ centered at the origin with radius $(2s)^{-1/(s-2)}$. By our scaling in z-direction we will see a different behavior for $\check{\rho}$. Depending on the relative magnitudes of s and t it is possible for the support of $\check{\rho}$ to diverge in z-direction. The exact relation between these parameter which we would need to determine the respective cases depends on the knowledge of the explicit form of $\rho^{\mathrm{TF}}_{\gamma,1}$, i.e. the explicit dependence of $\mu^{\mathrm{TF}}_{\gamma,1}$ on s and t. In general this is not known but we can give an approximate relation by using the asymptotics of the TF energy (4.25). By scaling the associated trial function (4.24) as in (4.28) we see that the support of $\check{\rho}$ stays bounded if $s > \frac{3t^2}{4t+3}$.

To illustrate this case we take $s = 6$ and $t = 8$ for figures 16- 18. All the following graphs will have a gray scaling of their own due to the great differences in the maximal density. This means that the value of $\check{\rho}$ at the darkest shade of gray is given by $\rho_{\max}$.

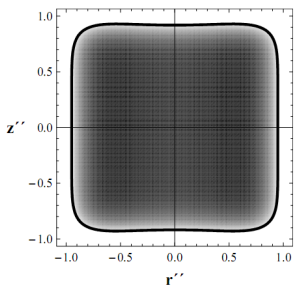

Fig. 16: $\Omega = 1$, $\rho_{\max} = 0.277$

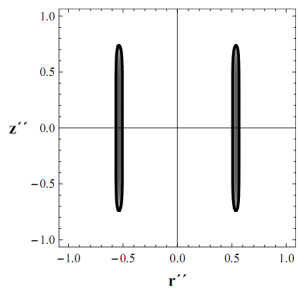

Fig. 17: $\Omega = 10^2$, $\rho_{\max} = 5.889$

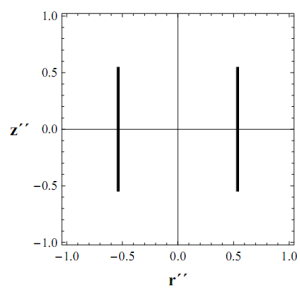

Fig. 18: $\Omega = 10^6$, $\rho_{\max} = 8310$

The support's divergence in z-direction is shown for $s = 6$ and $t = 10$ in Fig. 19-21.

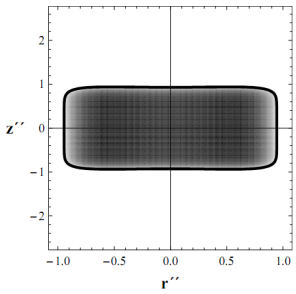

Fig. 19: $\Omega = 1$, $\rho_{\max} = 0.269$

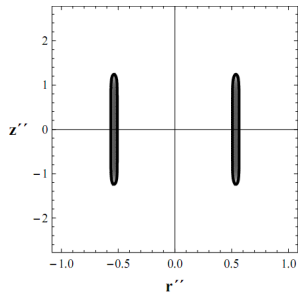

Fig. 20: $\Omega = 10^2$, $\rho_{\max} = 3.438$

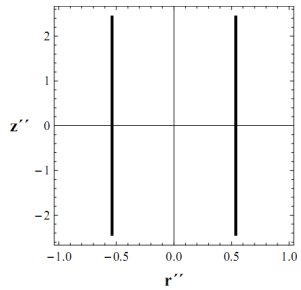

Fig. 21: $\Omega = 10^6$, $\rho_{\max} = 1769$

This concludes our illustrations on the TF density and we will continue with the main task of proving the asymptotics of the GP energy.

5 The TF Limit of the GP Functional

In this section we derive the asymptotics of the GP energy as g and possibly Ω tend to infinity. The different scalings in section 3.3 already outlined the cases that arise. We will obtain several limits depending on the asymptotic value of ω and the relative magnitude of s and t.

5.1 TF Limit for $\omega < \infty$

In the case of a dominating interaction energy contribution to the GP energy we have to take account of the vortex lattice that arises with rapid rotations. In the proof of the following theorem a first order approximation on its spacing will be given.

Theorem 5.1 (GP energy asymptotics for $\omega < \infty$) *Using the notation and relations prepared in sections 3.3 and 4.1 we demand that ω either vanishes or stays fixed (and finite) in the TF limit (i.e. $g \to \infty$). It then follows that the GP energy is asymptotically*

$$g^{-st/\sigma} E^{\mathrm{GP}}_{g,\Omega} = E^{\mathrm{TF}}_{1,\omega} + \begin{cases} O\Big(g^{-(s+2)t/(2\sigma)} \log g\Big) & \text{if } s > t \ \wedge \ t \geq 1 \\ O\Big(g^{-(s+2)t^2/(2\sigma)}\Big) & \text{if } s > t \ \wedge \ t < 1 \\ O\Big(g^{-s(t+2)/(2\sigma)} \log g\Big) & \text{if } s \leq t \end{cases} \tag{5.1}$$

with $\omega \equiv \Omega g^{-(s-2)t/(2\sigma)}$ and $\sigma \equiv s + (s+2)t$.

Proof:

In the following we will denote with C_ω a positive constant that is dependent on the value of ω but *independent* of $\underline{\varepsilon}$ or $\bar{\varepsilon}$. It can change its value from line to line and is not meant to be global variable.

We prove this theorem by calculating suitable lower and upper bounds on the GP functional following [BCPY08] and [CRDY07a]. The lower bound can be trivially found by ignoring the contributions of the positive magnetic-kinetic energy term and we immediately get

$$g^{-st/\sigma} E^{\mathrm{GP}}_{g,\Omega} \geq E^{\mathrm{TF}}_{1,\omega}.$$

For the upper bound we have to evaluate the GP functionals (3.14) and (3.16) on a trial function of the form

$$\tilde{\phi}(\vec{x}) = c_{\underline{\varepsilon}} \sqrt{\tilde{\varrho}_{\underline{\varepsilon}}(\vec{x})} \chi_{\underline{\varepsilon}}(\vec{r}) g_{\underline{\varepsilon}}(\vec{r}) \tag{5.2}$$

where $c_{\underline{\varepsilon}}$ is a normalization constant, $\tilde{\varrho}_{\underline{\varepsilon}}$ a regularization of the TF density, $g_{\underline{\varepsilon}}$ a phase factor and $\chi_{\underline{\varepsilon}}$ a function that vanishes at the singularities of $\vec{\nabla} g_{\underline{\varepsilon}}$. Functions $\chi_{\underline{\varepsilon}}$ and $g_{\underline{\varepsilon}}$ as well as $\tilde{\varrho}_{\underline{\varepsilon}}$ depend on $\underline{\varepsilon}$ and so does the normalization constant. We recall that $\underline{\varepsilon}$ is a negative power of g (see (3.13)) and thereby the TF limit corresponds to $\underline{\varepsilon} \to 0$.

The regularized density $\tilde{\varrho}_{\underline{\varepsilon}}$ is given by the convolution of the TF density $\rho^{\mathrm{TF}}_{1,\omega}$ with the function

$$j_{\underline{\varepsilon}}(\vec{x}) \equiv \frac{1}{8\pi \underline{\varepsilon}^3} \exp\left(-\frac{|\vec{x}|}{\underline{\varepsilon}}\right).$$

Since $\|j_{\underline{\varepsilon}}\|_1 = 1$ we see that $\sqrt{\tilde{\varrho}_{\underline{\varepsilon}}}$ is bounded with respect to the L^2-norm. Furthermore $j_{\underline{\varepsilon}}$ becomes concentrated around the origin for decreasing $\underline{\varepsilon}$ and we have uniform convergence of $\tilde{\varrho}_{\underline{\varepsilon}}$ to $\rho^{\mathrm{TF}}_{1,\omega}$ as $\underline{\varepsilon} \to 0$, i.e.,

$$\left\|\tilde{\varrho}_{\underline{\varepsilon}} - \rho^{\mathrm{TF}}_{1,\omega}\right\|_\infty \leq \begin{cases} C_\omega \underline{\varepsilon} & \text{if } t \geq 1 \\ C_\omega \underline{\varepsilon}^t & \text{if } t \leq 1 \end{cases} \tag{5.3}$$

where the latter case stems from the fact that $\rho_{1,\omega}^{\mathrm{TF}}$ is not differentiable at $z = 0$ (for $t < 1$). As $s > 2$, the radial part of the TF density (see (4.4)) can be expanded in a Taylor series, whereas the gradient of $|z|^t$ diverges as $z \to 0$ and $t < 1$. Nevertheless the second case of (5.3) can be obtained by

$$\begin{aligned}\left|\rho_{1,\omega}^{\mathrm{TF}}(\vec{x}) - \int_{\mathbb{R}^3} \mathrm{d}\vec{y}\, j_{\underline{\varepsilon}}(\vec{y})\rho_{1,\omega}^{\mathrm{TF}}(\vec{x}-\vec{y})\right| &\leq C_\omega \underline{\varepsilon} + \tfrac{1}{16\pi}\int_{\mathbb{R}^3} \mathrm{d}\vec{y}\, e^{-|\vec{y}|}\left||z_{\vec{x}}|^t - |z_{\vec{x}} - \underline{\varepsilon} z_{\vec{y}}|^t\right| \\ &\leq C_\omega \underline{\varepsilon} + \tfrac{1}{16\pi}\int_{\mathbb{R}^3} \mathrm{d}\vec{y}\, e^{-|\vec{y}|}\,|\underline{\varepsilon} z_{\vec{y}}|^t \\ &\leq C_\omega \underline{\varepsilon}^t\end{aligned}$$

where we used that $|a-b|^t \leq |a|^t + |b|^t$ for $0 < t \leq 1$ by Jensen's inequality.

The support of $j_{\underline{\varepsilon}}$ is the whole space $\mathbb{R}^3$ and thus $\tilde{\varrho}_{\underline{\varepsilon}}$ is not compactly supported like $\rho_{1,\omega}^{\mathrm{TF}}$; nevertheless it decreases exponentially fast outside the support of the TF density, which we will denote with $\mathcal{S}$. Indeed, for $\vec{x} \notin \mathcal{S}$, we have

$$\tilde{\varrho}_{\underline{\varepsilon}}(\vec{x}) = \frac{1}{4\pi\underline{\varepsilon}^3}\int_{\mathcal{S}} \mathrm{d}\vec{x}'\, \left\{\exp\left(-\frac{|\vec{x}-\vec{x}'|}{\underline{\varepsilon}}\right)\rho_{1,\omega}^{\mathrm{TF}}(\vec{x}')\right\} \leq \frac{1}{4\pi\underline{\varepsilon}^3}\exp\left(-\frac{\mathrm{dist}\,(\vec{x},\mathcal{S})}{\underline{\varepsilon}}\right)\overbrace{\left\|\rho_{1,\omega}^{\mathrm{TF}}\right\|_1}^{=1}. \tag{5.4}$$

where $\mathrm{dist}\,(\vec{x},\mathcal{S})$ is the minimal distance between a point $\vec{x} \in \mathbb{R}^3$ and the set $\mathcal{S} \subset \mathbb{R}^3$. We finish our preliminary discussion of the regularized density with two estimates of its gradient. First, by using that $|\vec{\nabla} j_{\underline{\varepsilon}}| = \underline{\varepsilon}^{-1} j_{\underline{\varepsilon}}$, we easily get that

$$|\vec{\nabla}\tilde{\varrho}_{\underline{\varepsilon}}| = |(\vec{\nabla} j_{\underline{\varepsilon}}) \star \rho_{1,\omega}^{\mathrm{TF}}| \leq |\vec{\nabla} j_{\underline{\varepsilon}}| \star \rho_{1,\omega}^{\mathrm{TF}} = \underline{\varepsilon}^{-1}\tilde{\varrho}_{\underline{\varepsilon}}. \tag{5.5}$$

To obtain a bound on $\left\|\vec{\nabla}\tilde{\varrho}_{\underline{\varepsilon}}\right\|_1$, we use the boundedness of $\left\|\vec{\nabla}\rho_{1,\omega}^{\mathrm{TF}}\right\|_1$, i.e.,

$$\left\|\vec{\nabla}\tilde{\varrho}_{\underline{\varepsilon}}\right\|_1 \leq \int_{\mathbb{R}^3}\mathrm{d}\vec{x}\int_{\mathbb{R}^3}\mathrm{d}\vec{x}'\,|\vec{\nabla}\rho_{1,\omega}^{\mathrm{TF}}(\vec{x}-\vec{x}')|j_{\underline{\varepsilon}}(\vec{x}') = \left\|\vec{\nabla}\rho_{1,\omega}^{\mathrm{TF}}\right\|_1\|j_{\underline{\varepsilon}}\|_1 \leq C_\omega. \tag{5.6}$$

To simulate the characteristic vortex distribution we introduce a finite regular lattice $\mathcal{L}_{\underline{\varepsilon}}$, which can have either a triangular, rectangular or hexagonal pattern. It consists of points $\vec{r}_j$ in $\mathcal{P}$ and is confined to the support of $\rho_{1,\omega}^{\mathrm{TF}}$. Each point is the center of a lattice cell $Q_{\underline{\varepsilon}}^j$ and the spacing $\ell_{\underline{\varepsilon}}$ between two neighboring cells is chosen in a way such that the area of each cell $Q_{\underline{\varepsilon}}^j$ is

$$\left|Q_{\underline{\varepsilon}}^j\right| \equiv \frac{2\pi\underline{\varepsilon}}{\omega}. \tag{5.7}$$

This fixes the spacing to

$$\ell_{\underline{\varepsilon}} = C_\omega\sqrt{\underline{\varepsilon}} \tag{5.8}$$

and gives the number of lattice points as

$$N_{\underline{\varepsilon}} = \frac{C_\omega}{\underline{\varepsilon}}\left(1 + O(\sqrt{\underline{\varepsilon}})\right). \tag{5.9}$$

Identifying $\mathcal{P}$ with the complex plane $\mathbb{C}$ enables us to define the phase factor as[6]

$$g_{\underline{\varepsilon}}(\vec{r}) \equiv \prod_{\zeta_j \in \mathcal{L}_{\underline{\varepsilon}}} \frac{\zeta - \zeta_j}{|\zeta - \zeta_j|}. \tag{5.10}$$

[6]We denote with $\zeta = x + iy$ the equivalent of $\vec{r} = (x, y)$ in the complex plane.

The corresponding phase function is given by

$$\theta_{\underline{\varepsilon}}(\vec{r}) \equiv \sum_{\zeta_j \in \mathcal{L}_{\underline{\varepsilon}}} \arg(\zeta - \zeta_j) \tag{5.11}$$

such that $g_{\underline{\varepsilon}}(\vec{r}) = \exp(i\theta_{\underline{\varepsilon}}(\vec{r}))$.

The points ζ_j are the centers of the lattice cells defined in (5.7) and if we treat $g_{\underline{\varepsilon}}$ as a function on $\mathbb{R}^3$ we see that it carries a vortex line of degree 1 through every point of the lattice $\mathcal{L}_{\underline{\varepsilon}}$. To model the vanishing particle density close to vortex lines we introduce a cut-off function $\chi_{\underline{\varepsilon}}$ defined as

$$\chi_{\underline{\varepsilon}}(\vec{r}) \equiv \begin{cases} 1 & \text{if } |\vec{r} - \vec{r}_j| \geq \underline{\varepsilon} \quad \text{for all } \vec{r}_j \in \mathcal{L}_{\underline{\varepsilon}} \\ \dfrac{|\vec{r} - \vec{r}_j|}{\underline{\varepsilon}} & \text{if } |\vec{r} - \vec{r}_j| \leq \underline{\varepsilon}. \end{cases} \tag{5.12}$$

It is clear that this function vanishes at every lattice point and is 1 outside the union of balls $\mathcal{B}^j_{\underline{\varepsilon}}$ with radius $\underline{\varepsilon}$ centered at these points. Note that this function will mitigate the mathematical difficulties that would arise from the singularities of $\vec{\nabla} g_{\underline{\varepsilon}}$ at the lattice points.

We should mention that additional accuracies in regard to experimental data, such as a strictly hexagonal pattern or bended vortex lines have no influence on the orders of the approximation we examine; nevertheless they will come into play if one wants to determine higher orders.

Prior to investigating the energy of the trial function, we derive lower and upper bounds for the normalization constant $c_{\underline{\varepsilon}}$. By $\|\tilde{\phi}\|_2 = 1$ and the fact that $|\chi_{\underline{\varepsilon}}(\vec{r}) g_{\underline{\varepsilon}}(\vec{r})| \leq 1$ on $\mathbb{R}^2$ we get that

$$\begin{aligned} 1 &= c_{\underline{\varepsilon}}^2 \int_{\mathbb{R}^3} \mathrm{d}\vec{x}\, \tilde{\varrho}_{\underline{\varepsilon}}(\vec{x})\, |\chi_{\underline{\varepsilon}}(\vec{r}) g_{\underline{\varepsilon}}(\vec{r})|^2 \\ &\leq c_{\underline{\varepsilon}}^2 \|\tilde{\varrho}_{\underline{\varepsilon}}\|_1 = c_{\underline{\varepsilon}}^2 \|j_{\underline{\varepsilon}} \star \rho^{\mathrm{TF}}_{1,\omega}\|_1 \\ &\overset{\text{Young}}{\leq} c_{\underline{\varepsilon}}^2 \|j_{\underline{\varepsilon}}\|_1 \|\rho^{\mathrm{TF}}_{1,\omega}\|_1 = c_{\underline{\varepsilon}}^2. \end{aligned}$$

The upper bound can be derived by omitting the contributions by the regions $\cup\mathcal{B}$ where $\chi_{\underline{\varepsilon}} < 1$ and using the trivial bound

$$\int_{\mathbb{R}} \mathrm{d}z\, \tilde{\varrho}_{\underline{\varepsilon}} \leq C_\omega. \tag{5.13}$$

This leads to

$$\begin{aligned} 1 &\geq c_{\underline{\varepsilon}}^2 \int_{\mathbb{R}^2 \setminus \cup\mathcal{B}} \mathrm{d}\vec{r} \int_{\mathbb{R}} \mathrm{d}z\, \tilde{\varrho}_{\underline{\varepsilon}}(\vec{x}) = c_{\underline{\varepsilon}}^2 \|\tilde{\varrho}_{\underline{\varepsilon}}\|_1 - c_{\underline{\varepsilon}}^2 \int_{\cup\mathcal{B}} \mathrm{d}\vec{r} \int_{\mathbb{R}} \mathrm{d}z\, \tilde{\varrho}_{\underline{\varepsilon}} \\ &\geq c_{\underline{\varepsilon}}^2 \left(1 - C_\omega \underline{\varepsilon}^2 N_{\underline{\varepsilon}}\right) \\ &\geq c_{\underline{\varepsilon}}^2 \left(1 - C_\omega \underline{\varepsilon}\right) \end{aligned}$$

and by Taylor expansion of $(1-x)^{-1}$ we get

$$c_{\underline{\varepsilon}}^2 \leq 1 + C_\omega \underline{\varepsilon}$$

Combining the two results yields the desired bounds on the normalization constant

$$1 \leq c_{\underline{\varepsilon}}^2 \leq 1 + C_\omega \underline{\varepsilon}. \tag{5.14}$$

We now proceed with the main part of the proof — the evaluation of the scaled GP functional on the trial function $\tilde{\phi}$. As we have two different functionals to consider, namely (3.14) and (3.16),

it is convenient to use a special notation. A term in angle brackets $\langle\cdot\rangle$ will denote a value that is only applicable for one of these two functionals, i.e.,

$$\langle\bar{\varepsilon}^{\,\beta}\rangle\vec{\nabla}_{\vec{r}} + \langle\underline{\varepsilon}^{\alpha}\rangle\vec{\nabla}_z \tag{5.15}$$

means that the terms $\bar{\varepsilon}^{\,\beta}$ and $\underline{\varepsilon}^{\alpha}$ are only used by one of the functionals. We will explicitly separate these cases if their treatment differ substantially. Otherwise consult (3.14) and (3.16) to look up to which functional a given term belongs. We furthermore recall that both $\underline{\varepsilon}$ and $\bar{\varepsilon}$ tend to 0 for large g and that the exponents α and β are positive in their respective cases.

The functionals evaluate to

$$\begin{aligned}\mathcal{E}^{\mathrm{GP}}_{\langle\underline{\varepsilon},\bar{\varepsilon}\rangle,\omega}[\tilde{\phi}] &= c_{\underline{\varepsilon}}^2\int_{\mathbb{R}^3}\mathrm{d}\vec{x}\,\left\{\left|\vec{\nabla}'\left(\sqrt{\tilde{\varrho}_{\underline{\varepsilon}}}\chi_{\underline{\varepsilon}}\right)g_{\underline{\varepsilon}}+\sqrt{\tilde{\varrho}_{\underline{\varepsilon}}}\chi_{\underline{\varepsilon}}\left(\vec{\nabla}'-i\vec{A}_{\omega/\langle\underline{\varepsilon},\bar{\varepsilon}\rangle}\right)g_{\underline{\varepsilon}}\right|^2\right\}+\langle\underline{\varepsilon}^{-2},\bar{\varepsilon}^{-2}\rangle\mathcal{E}^{\mathrm{TF}}_{1,\omega}[|\tilde{\phi}|^2]\\ &= \underbrace{c_{\underline{\varepsilon}}^2\int_{\mathbb{R}^3}\mathrm{d}\vec{x}\,\left|\vec{\nabla}'\left(\sqrt{\tilde{\varrho}_{\underline{\varepsilon}}}\chi_{\underline{\varepsilon}}\right)\right|^2}_{\mathbf{I}}+\underbrace{c_{\underline{\varepsilon}}^2\int_{\mathbb{R}^3}\mathrm{d}\vec{x}\,\left\{\tilde{\varrho}_{\underline{\varepsilon}}\chi_{\underline{\varepsilon}}^2\left|\left(\vec{\nabla}'-i\vec{A}_{\omega/\langle\underline{\varepsilon},\bar{\varepsilon}\rangle}\right)g_{\underline{\varepsilon}}\right|^2\right\}}_{\mathbf{II}}\\ &\qquad+\langle\underline{\varepsilon}^{-2},\bar{\varepsilon}^{-2}\rangle\underbrace{\mathcal{E}^{\mathrm{TF}}_{1,\omega}[|\tilde{\phi}|^2]}_{\mathbf{III}}\end{aligned} \tag{5.16}$$

where $\vec{\nabla}'$ denotes $\langle\bar{\varepsilon}^{\,\beta}\rangle\vec{\nabla}_{\vec{r}}+\langle\underline{\varepsilon}^{\alpha}\rangle\vec{\nabla}_z$. In the last equality we used that

$$\begin{aligned}&\left|\vec{\nabla}'\left(\sqrt{\tilde{\varrho}_{\underline{\varepsilon}}}\chi_{\underline{\varepsilon}}\right)g_{\underline{\varepsilon}}+\sqrt{\tilde{\varrho}_{\underline{\varepsilon}}}\chi_{\underline{\varepsilon}}\left(\vec{\nabla}'-i\vec{A}_{\omega/\langle\underline{\varepsilon},\bar{\varepsilon}\rangle}\right)g_{\underline{\varepsilon}}\right|^2\\ &\qquad=\left|\vec{\nabla}'\left(\sqrt{\tilde{\varrho}_{\underline{\varepsilon}}}\chi_{\underline{\varepsilon}}\right)+i\sqrt{\tilde{\varrho}_{\underline{\varepsilon}}}\chi_{\underline{\varepsilon}}\left(\vec{\nabla}'\theta_{\underline{\varepsilon}}-\vec{A}_{\omega/\langle\underline{\varepsilon},\bar{\varepsilon}\rangle}\right)\right|^2\underbrace{|g_{\underline{\varepsilon}}|^2}_{=1}\\ &\qquad=\left|\vec{\nabla}'\left(\sqrt{\tilde{\varrho}_{\underline{\varepsilon}}}\chi_{\underline{\varepsilon}}\right)\right|^2+\tilde{\varrho}_{\underline{\varepsilon}}\chi_{\underline{\varepsilon}}^2\left|\left(\vec{\nabla}'-i\vec{A}_{\omega/\langle\underline{\varepsilon},\bar{\varepsilon}\rangle}\right)g_{\underline{\varepsilon}}\right|^2/\underbrace{|ig_{\underline{\varepsilon}}|^2}_{=1}\end{aligned} \tag{5.17}$$

We will proceed to estimate the three terms **I**–**III** separately.

- **Estimate of I**

  Applying the product rule and $(a+b)^2\le 2a^2+2b^2$ we get

$$\mathbf{I}\le 2\int_{\mathbb{R}^3}\mathrm{d}\vec{x}\,\left|\vec{\nabla}'\sqrt{\tilde{\varrho}_{\underline{\varepsilon}}}\right|^2\chi_{\underline{\varepsilon}}^2+2\int_{\mathbb{R}^3}\mathrm{d}\vec{x}\,\tilde{\varrho}_{\underline{\varepsilon}}\left|\vec{\nabla}\chi_{\underline{\varepsilon}}\right|^2$$

  which can be easily estimated by

$$\int_{\mathbb{R}^3}\mathrm{d}\vec{x}\,\left|\vec{\nabla}'\sqrt{\tilde{\varrho}_{\underline{\varepsilon}}}\right|^2\chi_{\underline{\varepsilon}}^2\le\int_{\mathbb{R}^3}\mathrm{d}\vec{x}\,\left|\vec{\nabla}'\sqrt{\tilde{\varrho}_{\underline{\varepsilon}}}\right|^2\le\int_{\mathbb{R}^3}\mathrm{d}\vec{x}\,\frac{\left|\vec{\nabla}'\tilde{\varrho}_{\underline{\varepsilon}}\right|^2}{4\tilde{\varrho}_{\underline{\varepsilon}}}\overset{(5.5)}{\le}\frac{1}{4\underline{\varepsilon}}\left\|\vec{\nabla}'\tilde{\varrho}_{\underline{\varepsilon}}\right\|_1\overset{(5.6)}{\le}\frac{C_\omega}{\underline{\varepsilon}}$$

  and

$$\begin{aligned}\int_{\mathbb{R}^3}\mathrm{d}\vec{x}\,\tilde{\varrho}_{\underline{\varepsilon}}\left|\vec{\nabla}\chi_{\underline{\varepsilon}}\right|^2&=\int_{\mathbb{R}^2}\mathrm{d}\vec{r}\,\left|\vec{\nabla}\chi_{\underline{\varepsilon}}\right|^2\int_{\mathbb{R}^3}\mathrm{d}\vec{y}\,j_{\underline{\varepsilon}}(\vec{y})\underbrace{\int_{\mathbb{R}}\mathrm{d}z\,\rho^{\mathrm{TF}}_{1,\omega}(\vec{x}-\vec{y})}_{\le C_\omega}\\ &\le C_\omega\int_{\mathbb{R}^2}\mathrm{d}\vec{r}\,\left|\vec{\nabla}_{\vec{r}}\chi_{\underline{\varepsilon}}\right|^2=\underline{\varepsilon}^{-2}\int_{\cup\mathcal{B}}\mathrm{d}\vec{r}\,1\le C_\omega N_{\underline{\varepsilon}}\le\frac{C_\omega}{\underline{\varepsilon}}\end{aligned} \tag{5.18}$$

  yielding

$$\mathbf{I}\le\frac{C_\omega}{\underline{\varepsilon}}. \tag{5.19}$$

  We denote with $\cup\mathcal{B}$ the union of all discs $\mathcal{B}_{\underline{\varepsilon}}^j$ (centered at lattice points $\vec{r}_j\in\mathcal{L}_{\underline{\varepsilon}}$ with radius $\underline{\varepsilon}$).

- **Estimate of II**

This term incorporates the energy contribution of the vortices, which we will estimate by splitting the domain of integration into several parts, where we can treat the integrals differently. The motivation for such a procedure mainly stems from two properties of the trial function. Firstly, the intersection points of the vortex lines with $\mathcal{P}$ (see (4.12)) are confined to the support of the TF density $\rho^{\mathrm{TF}}_{1,\omega}$. Secondly, the regularization of the TF density $\tilde{\varrho}_{\underline{\varepsilon}}$ is exponentially small in $\underline{\varepsilon}$ if evaluated at a point outside the support $\mathcal{S}$ of $\rho^{\mathrm{TF}}_{1,\omega}$ (see (5.4)).

The phase factor $g_{\underline{\varepsilon}}$ and the cut-off function $\chi_{\underline{\varepsilon}}$, while functions on $\mathbb{R}^3$, do not vary in z-direction and thus it will be convenient to project the required subsets of $\mathbb{R}^3$ onto $\mathcal{P}$ and denote them by $\cdot_{\mathrm{2D}}$. Furthermore we will use the notation $\cdot_{\mathrm{cyl}}$ for the Cartesian product of a subset of $\mathcal{P}$ with the z-axis. This gives us the following definitions

$$\begin{aligned} \mathcal{S} &\equiv \overline{\left\{\vec{x} \in \mathbb{R}^3 \middle| \rho^{\mathrm{TF}}_{1,\omega}(\vec{x}) > 0\right\}} \\ \mathcal{S}_{\mathrm{2D}} &\equiv \left\{\vec{r} \in \mathbb{R}^2 \middle| (\vec{r}, 0) \in \mathcal{S}\right\} \\ \mathcal{S}_{\mathrm{cyl}} &\equiv \left\{(\vec{r}, z) \in \mathbb{R}^3 \middle| \vec{r} \in \mathcal{S}_{\mathrm{2D}}\right\} \end{aligned} \tag{5.20}$$

and we note that all vortex lines are contained in $\mathcal{S}_{\mathrm{cyl}}$. The exponential smallness of $\tilde{\varrho}_{\underline{\varepsilon}}$ can only be utilized on a subset of $\mathbb{R}^3$ which has positive distance from $\mathcal{S}$. Thus it will be necessary add a small neighborhood to the support of $\rho^{\mathrm{TF}}_{1,\omega}$ and use its complement. The neighborhoods are given by

$$\begin{aligned} \mathcal{O} &\equiv \left\{\vec{x} \in \mathbb{R}^3 \middle| 0 < \operatorname{dist}(\vec{x}, \mathcal{S}) \leq C\sqrt{\underline{\varepsilon}}\right\} \\ \mathcal{O}_{\mathrm{2D}} &\equiv \left\{\vec{r} \in \mathbb{R}^2 \middle| (\vec{r}, 0) \in \mathcal{O}\right\} = \left\{\vec{r} \in \mathbb{R}^2 \middle| 0 < \operatorname{dist}(\vec{r}, \mathcal{S}_{\mathrm{2D}}) \leq C\sqrt{\underline{\varepsilon}}\right\} \\ \mathcal{O}_{\mathrm{cyl}} &\equiv \left\{(\vec{r}, z) \in \mathbb{R}^3 \middle| \vec{r} \in \mathcal{O}_{\mathrm{2D}}\right\} = \left\{(\vec{r}, z) \in \mathbb{R}^3 \middle| 0 < \operatorname{dist}(\vec{r}, \mathcal{S}_{\mathrm{2D}}) \leq C\sqrt{\underline{\varepsilon}}\right\} \end{aligned} \tag{5.21}$$

and we will mainly use the complementary sets $\mathbb{R}^3 \setminus (\mathcal{S} \cup \mathcal{O})$, $\mathbb{R}^2 \setminus (\mathcal{S}_{\mathrm{2D}} \cup \mathcal{O}_{\mathrm{2D}})$ and $\mathbb{R}^3 \setminus (\mathcal{S}_{\mathrm{cyl}} \cup \mathcal{O}_{\mathrm{cyl}})$, all of which allow us to use (5.4). The constant C is chosen as a small fraction of the scaled cell spacing $\ell_{\underline{\varepsilon}}\underline{\varepsilon}$ such that $\mathcal{O}_{\mathrm{2D}}$ is covered by the cells as $\underline{\varepsilon} \to 0$.

Now we are set to split the domain of integration and write

$$\begin{aligned} \mathbf{II} \leq &\int_{\mathcal{S}_{\mathrm{cyl}} \cup \mathcal{O}_{\mathrm{cyl}}} \mathrm{d}\vec{x}\, \tilde{\varrho}_{\underline{\varepsilon}} \chi^2_{\underline{\varepsilon}} \left| \left(\langle \bar{\varepsilon}^{\,\beta} \rangle \vec{\nabla}_{\vec{r}} - i\vec{A}_{\omega/\langle \underline{\varepsilon}, \bar{\varepsilon} \rangle}\right) g_{\underline{\varepsilon}} \right|^2 \\ &+ \int_{\mathbb{R}^3 \setminus (\mathcal{S}_{\mathrm{cyl}} \cup \mathcal{O}_{\mathrm{cyl}})} \mathrm{d}\vec{x}\, \tilde{\varrho}_{\underline{\varepsilon}} \left| \left(\langle \bar{\varepsilon}^{\,\beta} \rangle \vec{\nabla}_{\vec{r}} - i\vec{A}_{\omega/\langle \underline{\varepsilon}, \bar{\varepsilon} \rangle}\right) g_{\underline{\varepsilon}} \right|^2 \end{aligned} \tag{5.22}$$

where $\vec{\nabla}_{\vec{r}}$ denotes $(\partial_x, \partial_y, 0)$. To examine the last integral we need two preliminary estimates. Using $(a+b)^2 \leq 2a^2 + 2b^2$ earns us

$$\begin{aligned} \left| \left(\langle \bar{\varepsilon}^{\,\beta} \rangle \vec{\nabla}_{\vec{r}} - i\vec{A}_{\omega/\langle \underline{\varepsilon}, \bar{\varepsilon} \rangle}\right) g_{\underline{\varepsilon}} \right|^2 &\leq 2\langle \bar{\varepsilon}^{\,2\beta} \rangle \left| \vec{\nabla}_{\vec{r}} g_{\underline{\varepsilon}} \right|^2 + 2 \left| \vec{A}_{\omega/\langle \underline{\varepsilon}, \bar{\varepsilon} \rangle} g_{\underline{\varepsilon}} \right|^2 \\ &\leq 2\langle \bar{\varepsilon}^{\,2\beta} \rangle \left| \vec{\nabla}_{\vec{r}} g_{\underline{\varepsilon}} \right|^2 + C_\omega \langle \underline{\varepsilon}^{-2}, \bar{\varepsilon}^{\,-2} \rangle \left| \vec{r} \right|^2 . \end{aligned} \tag{5.23}$$

On $\mathbb{R}^3 \setminus (\mathcal{S}_{\mathrm{cyl}} \cup \mathcal{O}_{\mathrm{cyl}})$ the gradient of the phase can be bounded by

$$\begin{aligned} \left| \vec{\nabla} g_{\underline{\varepsilon}}(\vec{r}) \right| &= \left| \sum_{\zeta_j \in \mathcal{L}_{\underline{\varepsilon}}} \vec{\nabla} \left(\frac{\zeta - \zeta_j}{|\zeta - \zeta_j|} \right) \prod_{j \neq k} \frac{\zeta - \zeta_k}{|\zeta - \zeta_k|} \right| \leq \sum_{\zeta_j \in \mathcal{L}_{\underline{\varepsilon}}} \left| \vec{\nabla} \left(\frac{\zeta - \zeta_j}{|\zeta - \zeta_j|} \right) \right| \\ &\leq \sum_{\vec{r}_j \in \mathcal{L}_{\underline{\varepsilon}}} \frac{1}{|\vec{r} - \vec{r}_j|} \leq N_{\underline{\varepsilon}} \left(\inf_{\vec{r}_j \in \mathcal{L}_{\underline{\varepsilon}}} |\vec{r} - \vec{r}_j| \right)^{-1} \leq C_\omega \frac{N_{\underline{\varepsilon}}}{\sqrt{\underline{\varepsilon}}} \overset{(5.9)}{\leq} C_\omega \underline{\varepsilon}^{-3/2} \end{aligned} \tag{5.24}$$

where the next to last inequality depends on or choice of $\mathcal{O}_{\mathrm{cyl}}$. Finally we are set to apply (5.4) and get

$$\begin{aligned}
&\int_{\mathbb{R}^3\setminus(\mathcal{S}_{\mathrm{cyl}}\cup\mathcal{O}_{\mathrm{cyl}})} \mathrm{d}\vec{x}\, \tilde{\varrho}_{\underline{\varepsilon}} \left|\left(\langle\bar{\varepsilon}^{\,\beta}\rangle\vec{\nabla}_{\vec{r}} - i\vec{A}_{\omega/\langle\underline{\varepsilon},\bar{\varepsilon}\rangle}\right) g_{\underline{\varepsilon}}\right|^2 \\
&\quad\leq \int_{\mathbb{R}^3\setminus(\mathcal{S}_{\mathrm{cyl}}\cup\mathcal{O}_{\mathrm{cyl}})} \mathrm{d}\vec{x}\, \left(C_\omega\langle\bar{\varepsilon}^{\,2\beta}\rangle\underline{\varepsilon}^{-3} + C'_\omega\langle\underline{\varepsilon}^{-2},\bar{\varepsilon}^{\,-2}\rangle\,|\vec{r}\,|^2\right)\frac{1}{\underline{\varepsilon}^3}\exp\left\{-\frac{\mathrm{dist}\,(\vec{x},\mathcal{S})}{\underline{\varepsilon}}\right\} \\
&\quad\leq \int_{\mathbb{R}^3\setminus(\mathcal{S}\cup\mathcal{O})} \mathrm{d}\vec{x}\, \left(C_\omega\langle\bar{\varepsilon}^{\,2\beta}\rangle\underline{\varepsilon}^{-3} + C'_\omega\langle\underline{\varepsilon}^{-2},\bar{\varepsilon}^{\,-2}\rangle\,|\vec{r}\,|^2\right)\frac{1}{\underline{\varepsilon}^3}\exp\left\{-\frac{\mathrm{dist}\,(\vec{x},\mathcal{S})}{\underline{\varepsilon}}\right\}.
\end{aligned} \tag{5.25}$$

For the last inequality we used that $\mathcal{S}\cup\mathcal{O}\subset\mathcal{S}_{\mathrm{cyl}}\cup\mathcal{O}_{\mathrm{cyl}}$ and that the integrand is non-negative. If we take all points with distance d from $\mathcal{S}$, we see that the exponential term evaluates to $e^{d/\underline{\varepsilon}}$ on this surface. We have already shown in section 4 that the support of $\rho^{\mathrm{TF}}_{1,\omega}$ is compact and its envelope $\mathcal{E}$ - when treated as a two-dimensional surface in $\mathbb{R}^3$ - is $\mathcal{C}^2$ almost everywhere and has a finite area which depends only on ω. This implies that Gaussian and mean curvature are finite everywhere on the surface save the ring (or rings) where it intersects $\mathcal{P}$, if $t\leq 1$. We then take all points with distance d from $\mathcal{E}$ on the outside of $\mathcal{E}$ and denote the new surface with $\mathcal{E}_d$. At a point $\vec{x}\in\mathcal{E}$ where both curvatures are finite such a transition changes the area element around $\vec{x}$ as

$$\mathrm{d}A\,(\vec{x}+\vec{n}d) = \mathrm{d}A\,(\vec{x})\left(1+2Md+Gd^2\right), \qquad \vec{x}\in\mathcal{E},\ \kappa_1 d>-1,\ \kappa_2 d>-1 \tag{5.26}$$

where $\vec{n}$ is the unit normal in point $\vec{x}$ (pointing outwards) whereas κ_1 and κ_2 are the principal curvatures of $\mathcal{E}$ in $\vec{x}$. This gives us the mean curvature as $M=(\kappa_1+\kappa_1)/2$ and Gaussian curvature as $G=\kappa_1\kappa_2$.

As already indicated by the constraints $\kappa_i d\geq -1$ we have to take a closer look at the case of a negative principal curvature in a point $\vec{x}$. A negative value of κ_i would shrink the surface in the principal direction of κ_i as we increase d. The principal curvature of the new surface in point $\vec{x}+\vec{n}d$ is given by $\kappa_i/(1+\kappa_i d)$ which diverges as $\kappa_i d\to -1$. In the limit case a sharp edge arises that 'points' in direction of $-\vec{n}$. A further increase in d thus leads to an areal growth that is less than given in (5.26) because self intersection of $\mathcal{E}_d$ are not allowed.

In the case of $t\leq 1$ (see section 4.3) we have one or two rings in $\mathcal{P}$ at which $\mathcal{E}$ has infinite mean and Gaussian curvature. To expand the surface we take all points with distance d from these rings; the area of the resulting surface is clearly smaller than the surface area of tori with inner radii d around those rings. Thus we get an upper bound on the expanded surface's area, namely $4\pi^2 d(R_{\mathrm{in}}+R_{\mathrm{out}})\leq C_\omega d$.

Summarizing the last evaluations, we have seen the area of the surface $\mathcal{E}_d$, consisting of all points with distance d from $\mathcal{S}$, can be bounded by $C_\omega(1+d+d^2)$. We will use this result to evaluate the integral (5.25). The domain of integration, $\mathbb{R}^3\setminus(\mathcal{S}\cup\mathcal{O})$, can be partitioned into shells of constant distance d from $(\mathcal{S}\cup\mathcal{O})$. On a shell with distance d the exponential term of (5.25) evaluates to the constant value $e^{-d/\underline{\varepsilon}}$ and we can bound $|\vec{r}\,|^2$ by $(R_{\mathrm{out}}+d)^2$. Such a procedure yields

$$\begin{aligned}
&\int_{\mathbb{R}^3\setminus(\mathcal{S}\cup\mathcal{O})} \mathrm{d}\vec{x}\, \tilde{\varrho}_{\underline{\varepsilon}} \left|\left(\langle\bar{\varepsilon}^{\,\beta}\rangle\vec{\nabla}_{\vec{r}} - i\vec{A}_{\omega/\langle\underline{\varepsilon},\bar{\varepsilon}\rangle}\right) g_{\underline{\varepsilon}}\right|^2 \\
&\qquad\qquad \leq \frac{C_\omega}{\underline{\varepsilon}^3}\int_{C\sqrt{\underline{\varepsilon}}}^{\infty} \mathrm{d}d\,(1+d+d^2)\left(\langle\bar{\varepsilon}^{\,2\beta}\rangle\underline{\varepsilon}^{-3} + \langle\underline{\varepsilon}^{-2},\bar{\varepsilon}^{\,-2}\rangle(R_{\mathrm{out}}+d)^2\right)e^{-d/\underline{\varepsilon}}
\end{aligned}$$

which evaluates to

$$\leq C_\omega \sum (\underline{\varepsilon}, \bar{\varepsilon}\,, \underline{\varepsilon}) e^{-C/\sqrt{\underline{\varepsilon}}} \tag{5.27}$$

where $\sum(\dots)$ is a finite sum of arbitrary powers of the given arguments. In our desired limit this sum does not matter since the whole expression vanishes exponentially fast as $\underline{\varepsilon} \to 0$. Such a bound suffices for our needs and we proceed to estimate the integral over $\mathcal{S}_{\text{cyl}} \cup \mathcal{O}_{\text{cyl}}$ in (5.22). From (5.3) follows that

$$\begin{aligned}
&\int_{\mathcal{S}_{\text{cyl}} \cup \mathcal{O}_{\text{cyl}}} \mathrm{d}\vec{x}\, \tilde{\varrho}_{\underline{\varepsilon}} \chi_{\underline{\varepsilon}}^2 \left| \left(\langle \bar{\varepsilon}^{\,\beta} \rangle \vec{\nabla}_{\vec{r}} - i\vec{A}_{\omega/\langle \underline{\varepsilon}, \bar{\varepsilon} \rangle} \right) g_{\underline{\varepsilon}} \right|^2 \\
&\qquad \leq \left(1 + C_\omega \underline{\varepsilon}^{\min(1,t)} \right) \langle \bar{\varepsilon}^{\,\beta} \rangle \int_{\mathcal{S}_{\text{2D}} \cup \mathcal{O}_{\text{2D}}} \mathrm{d}\vec{r}\, \chi_{\underline{\varepsilon}}^2 \left| \left(\vec{\nabla}_{\vec{r}} - i\vec{A}_{\omega/\underline{\varepsilon}} \right) g_{\underline{\varepsilon}} \right|^2 \underbrace{\int_{\mathbb{R}} \mathrm{d}z\, \rho_{1,\omega}^{\text{TF}}}_{\equiv \rho_{1,\omega}^{\text{TF,2D}}}
\end{aligned} \tag{5.28}$$

and we are set to use proposition 5.3 which yields

$$\mathbf{II} \leq \langle \bar{\varepsilon}^{\,\beta} \rangle \left(\frac{\omega}{2} \frac{|\log \underline{\varepsilon}|}{\underline{\varepsilon}} + O(\underline{\varepsilon}^{-1}) \right). \tag{5.29}$$

- **Estimate of III**

  In this part we show the convergence of the TF functional on the trial function, $\mathcal{E}_{1,\omega}^{\text{TF}} \left[|\tilde{\phi}|^2 \right]$, to the actual TF energy $E_{1,\omega}^{\text{TF}}$ in the limit $\underline{\varepsilon} \to 0$. We will achieve this by an intermediate step, namely the evaluation of the TF functional on the regularized TF density, e.g.,

$$\mathcal{E}_{1,\omega}^{\text{TF}} \left[|\tilde{\phi}|^2 \right] - E_{1,\omega}^{\text{TF}} = \mathcal{E}_{1,\omega}^{\text{TF}} \left[|\tilde{\phi}|^2 \right] - \mathcal{E}_{1,\omega}^{\text{TF}} \left[\tilde{\varrho}_{\underline{\varepsilon}} \right] + \mathcal{E}_{1,\omega}^{\text{TF}} \left[\tilde{\varrho}_{\underline{\varepsilon}} \right] - \underbrace{\mathcal{E}_{1,\omega}^{\text{TF}} \left[\rho_{1,\omega}^{\text{TF}} \right]}_{= E_{1,\omega}^{\text{TF}}}. \tag{5.30}$$

In the treatment of the difference of the first two terms our previously established bounds on $c_{\underline{\varepsilon}}$ (see (5.14)) become handy. By defining with

$$W_\omega(r,z) \equiv r^s - \tfrac{1}{4}\omega^2 r^2 + |z|^t$$

an effective potential we can write

$$\begin{aligned}
\mathcal{E}_{1,\omega}^{\text{TF}} \left[|\tilde{\phi}|^2 \right] - \mathcal{E}_{1,\omega}^{\text{TF}} \left[\tilde{\varrho}_{\underline{\varepsilon}} \right] &= \int_{\mathbb{R}^3} \mathrm{d}\vec{x}\, \left\{ W_\omega \tilde{\varrho}_{\underline{\varepsilon}} \left(c_{\underline{\varepsilon}}^2 \left| \chi_{\underline{\varepsilon}} g_{\underline{\varepsilon}} \right|^2 - 1 \right) + \tilde{\varrho}_{\underline{\varepsilon}}^2 \left(c_{\underline{\varepsilon}}^4 \left| \chi_{\underline{\varepsilon}} g_{\underline{\varepsilon}} \right|^4 - 1 \right) \right\} \\
&\leq \int_{\mathbb{R}^3} \mathrm{d}\vec{x}\, \left\{ W_\omega \tilde{\varrho}_{\underline{\varepsilon}} \left(c_{\underline{\varepsilon}}^2 - 1 \right) + \tilde{\varrho}_{\underline{\varepsilon}}^2 \left(c_{\underline{\varepsilon}}^4 - 1 \right) \right\} \\
&\overset{(5.14)}{\leq} C_\omega \underline{\varepsilon} \int_{\mathbb{R}^3} \mathrm{d}\vec{x}\, \left\{ W_\omega \tilde{\varrho}_{\underline{\varepsilon}} + \tilde{\varrho}_{\underline{\varepsilon}}^2 \right\} \\
&= C_\omega \underline{\varepsilon}\, \mathcal{E}_{1,\omega}^{\text{TF}} \left[\tilde{\varrho}_{\underline{\varepsilon}} \right] \\
&= C_\omega \underline{\varepsilon} \left(\mathcal{E}_{1,\omega}^{\text{TF}} \left[\tilde{\varrho}_{\underline{\varepsilon}} \right] - E_{1,\omega}^{\text{TF}} \right) + C'_\omega \underline{\varepsilon}
\end{aligned} \tag{5.31}$$

The first summand of (5.31) and the second difference in (5.30) can be bounded by applying already developed methods. To evaluate

$$\mathcal{E}_{1,\omega}^{\text{TF}} \left[\tilde{\varrho}_{\underline{\varepsilon}} \right] - E_{1,\omega}^{\text{TF}} = \int_{\mathbb{R}^3} \mathrm{d}\vec{x}\, \left\{ W_\omega \left(\tilde{\varrho}_{\underline{\varepsilon}} - \rho_{1,\omega}^{\text{TF}} \right) + \tilde{\varrho}_{\underline{\varepsilon}}^2 - \rho_{1,\omega}^{\text{TF}\,2} \right\}$$

we have to split the domain of integration in the same manner as in the estimate of **II**. Here, we will use the sets $\mathcal{S} \cup \mathcal{O}$ and $\mathbb{R}^3 \setminus (\mathcal{S} \cup \mathcal{O})$. On the first set we can use (5.3) while on the second set the inequality (5.4).

The interaction term evaluates to

$$\begin{aligned}\int_{\mathbb{R}^3} \mathrm{d}\vec{x}\, \left(\tilde{\varrho}_{\underline{\varepsilon}}^2 - \rho_{1,\omega}^{\mathrm{TF}\,2}\right) &= \int_{\mathcal{S}\cup\mathcal{O}} \mathrm{d}\vec{x}\, \left(\tilde{\varrho}_{\underline{\varepsilon}} - \rho_{1,\omega}^{\mathrm{TF}}\right)\left(\tilde{\varrho}_{\underline{\varepsilon}} + \rho_{1,\omega}^{\mathrm{TF}}\right) + \int_{\mathbb{R}^3\setminus(\mathcal{S}\cup\mathcal{O})} \mathrm{d}\vec{x}\, \tilde{\varrho}_{\underline{\varepsilon}}^2 \\ &\leq 2\left\|\tilde{\varrho}_{\underline{\varepsilon}} - \rho_{1,\omega}^{\mathrm{TF}}\right\|_\infty + C_\omega \left\|\tilde{\varrho}_{\underline{\varepsilon}} - \rho_{1,\omega}^{\mathrm{TF}}\right\|_\infty^2 + C'_\omega \sum(\underline{\varepsilon}) e^{-2/\sqrt{\underline{\varepsilon}}} \\ &\leq C_\omega \underline{\varepsilon}^{\min(1,t)} \end{aligned} \tag{5.32}$$

where $\sum(\underline{\varepsilon})$ is defined as in (5.27). The remaining integral is estimated by shifting the regularizing function $j_{\underline{\varepsilon}}$ onto the effective potential and using its regularity. We see that

$$\begin{aligned}\int_{\mathbb{R}^3} \mathrm{d}\vec{x}\, W_\omega \left(\tilde{\varrho}_{\underline{\varepsilon}} - \rho_{1,\omega}^{\mathrm{TF}}\right) &= \int_{\mathcal{S}} \mathrm{d}\vec{x}\, \rho_{1,\omega}^{\mathrm{TF}} \left(j_{\underline{\varepsilon}} \star W_\omega - W_\omega\right) \\ &\leq \frac{1}{8\pi} \int_{\mathcal{S}} \mathrm{d}\vec{x}\, \rho_{1,\omega}^{\mathrm{TF}}(\vec{x}) \int_{\mathbb{R}^3} \mathrm{d}\vec{y}\, e^{-|\vec{y}|} \left|W_\omega(\vec{x} - \underline{\varepsilon}\vec{y}) - W_\omega(\vec{x})\right| \end{aligned}$$

where the estimate of the last term depends on the value of t. For $t > 1$ the potential $W_\omega(r, z)$ is differentiable with

$$W_\omega(\vec{x} - \underline{\varepsilon}\vec{y}) - W_\omega(\vec{x}) = \underline{\varepsilon}\vec{y} \cdot \vec{\nabla} W_\omega(\vec{x}) + O(\underline{\varepsilon}^2)$$

whereas for $t < 1$ it exhibits the same kind of non-differentiability as $\rho_{1,\omega}^{\mathrm{TF}}$. With essentially the same calculation as in (5.3) we get

$$\int_{\mathbb{R}^3} \mathrm{d}\vec{x}\, W_\omega \left(\tilde{\varrho}_{\underline{\varepsilon}} - \rho_{1,\omega}^{\mathrm{TF}}\right) \leq \begin{cases} C_\omega \underline{\varepsilon} & \text{if } t \geq 1 \\ C_\omega \underline{\varepsilon}^t & \text{if } t \leq 1. \end{cases} \tag{5.33}$$

By combining (5.31), (5.32) and (5.33) we obtain the overall convergence

$$\begin{aligned}\mathcal{E}_{1,\omega}^{\mathrm{TF}}\left[\left|\tilde{\phi}\right|^2\right] - E_{1,\omega}^{\mathrm{TF}} &\leq C_\omega \underline{\varepsilon}^{\min(t+1,2)} + C'_\omega \underline{\varepsilon}^{\min(t,1)} + C''_\omega \underline{\varepsilon} \\ &\leq C_\omega \underline{\varepsilon}^{\min(t,1)}. \end{aligned} \tag{5.34}$$

This concludes our treatment of **I**–**III** and we collect our labor's fruits. The three estimates (5.19), (5.29) and (5.34) together with the bound on the normalization constant (5.14) yield

$$\begin{aligned}\mathcal{E}_{\langle\underline{\varepsilon},\bar{\varepsilon}\rangle,\omega}^{\mathrm{GP}}[\tilde{\phi}] \leq (1 + C_\omega \underline{\varepsilon}) &\left(C'_\omega \underline{\varepsilon}^{-1} + \langle \bar{\varepsilon}^{\,\beta}\rangle \frac{\omega}{2} \frac{|\log \underline{\varepsilon}|}{\underline{\varepsilon}} + C''_\omega \langle \bar{\varepsilon}^{\,\beta}\rangle \underline{\varepsilon}^{-1}\right) \\ &+ \langle \underline{\varepsilon}^{-2}, \bar{\varepsilon}^{\,-2}\rangle \left(E_{1,\omega}^{\mathrm{TF}} + C'''_\omega \underline{\varepsilon}^{\min(t,1)}\right) \end{aligned}$$

which implies in the case of $s > t$

$$\begin{aligned} \underline{\varepsilon}^2 \mathcal{E}_{\underline{\varepsilon},\omega}^{\mathrm{GP}}[\tilde{\phi}] &\leq E_{1,\omega}^{\mathrm{TF}} + \tfrac{\omega}{2}\underline{\varepsilon}\,|\log \underline{\varepsilon}| + C_\omega \underline{\varepsilon} && \text{if } t \geq 1 \\ \underline{\varepsilon}^2 \mathcal{E}_{\underline{\varepsilon},\omega}^{\mathrm{GP}}[\tilde{\phi}] &\leq E_{1,\omega}^{\mathrm{TF}} + C_\omega \underline{\varepsilon}^t && \text{if } t \leq 1. \end{aligned}$$

If $t > s$ we can use that $\bar{\varepsilon}^{\beta+2}\underline{\varepsilon}^{-1} = \bar{\varepsilon}$ and obtain

$$\bar{\varepsilon}^{\,2}\bar{\mathcal{E}}^{\mathrm{GP}}_{\bar{\varepsilon},\omega}[\tilde{\phi}] \leq E^{\mathrm{TF}}_{1,\omega} + \tfrac{\omega}{2}\bar{\varepsilon}\,|\log\underline{\varepsilon}| + C_\omega\bar{\varepsilon}\,.$$

Inserting the definitions for $\underline{\varepsilon}$, $\bar{\varepsilon}$ and the functionals gives

$$\begin{aligned}
g^{-st/\sigma}E^{\mathrm{GP}}_{g,\Omega} &\leq E^{\mathrm{TF}}_{1,\omega} + \frac{\omega}{2}\frac{(s+2)t}{2\sigma}g^{-(s+2)t/(2\sigma)}\log g + C_\omega g^{-(s+2)t/(2\sigma)} && \text{if } s > t \wedge t \geq 1\\
g^{-st/\sigma}E^{\mathrm{GP}}_{g,\Omega} &\leq E^{\mathrm{TF}}_{1,\omega} + C_\omega g^{-(s+2)t^2/(2\sigma)} && \text{if } s > t \wedge t < 1\\
g^{-st/\sigma}E^{\mathrm{GP}}_{g,\Omega} &\leq E^{\mathrm{TF}}_{1,\omega} + \frac{\omega}{2}\frac{(s+2)t}{2\sigma}g^{-s(t+2)/(2\sigma)}\log g + C_\omega g^{-s(t+2)/(2\sigma)} && \text{if } s < t
\end{aligned}$$

with $\omega \equiv \Omega g^{-(s-2)t/(2\sigma)}$ and $\sigma \equiv s + (s+2)t$.

□

This result can immediately be used to derive the asymptotics of the scaled GP minimizer $\phi^{\mathrm{GP}}_\omega$ given by

$$\phi^{\mathrm{GP}}_{g,\Omega}(\vec{r}, z) \equiv g^{-(s+2t)/(2\sigma)}\phi^{\mathrm{GP}}_\omega\left(g^{t/\sigma}\vec{r}, g^{s/\sigma}z\right). \tag{5.35}$$

Note that $\phi^{\mathrm{GP}}_\omega$ is the minimizer of the scaled GP functionals $\mathcal{E}^{\mathrm{GP}}_{\underline{\varepsilon},\omega}$ and $\bar{\mathcal{E}}^{\mathrm{GP}}_{\bar{\varepsilon},\omega}$.

Corollary 5.2 (GP density asymptotics for $\omega < \infty$) *With the same preconditions as in Theorem 5.1 we have*

$$\left\| \left|\phi^{\mathrm{GP}}_\omega\right|^2 - \rho^{\mathrm{TF}}_{1,\omega} \right\|_{L^2(\mathbb{R}^3)} = \begin{cases} O\left(g^{-(s+2)t/(2\sigma)}\log g\right) & \textit{if } s > t \wedge t \geq 1\\ O\left(g^{-(s+2)t^2/(2\sigma)}\right) & \textit{if } s > t \wedge t < 1\\ O\left(g^{-s(t+2)/(2\sigma)}\log g\right) & \textit{if } s \leq t \end{cases} \tag{5.36}$$

with $\omega \equiv \Omega g^{-(s-2)t/(2\sigma)}$ and $\sigma \equiv s + (s+2)t$.

Proof: Following the calculations in [CRDY07a, Col. 3.1] we define with

$$\varsigma(\vec{r}, z) \equiv \frac{1}{2}\left(\mu^{\mathrm{TF}}_{1,\omega} + \tfrac{1}{4}\omega r^2 - r^s - |z|^t\right)$$

a function equivalent with $\rho^{\mathrm{TF}}_{1,\omega}$ on the support of $\rho^{\mathrm{TF}}_{1,\omega}$. From the negativity of ς on all points outside the support we infer that

$$\int_{\mathbb{R}^3}\mathrm{d}\vec{x}\,\left(\left|\phi^{\mathrm{GP}}_\omega\right|^2 - \rho^{\mathrm{TF}}_{1,\omega}\right)^2 \leq \left\|\phi^{\mathrm{GP}}_\omega\right\|_4^4 + \left\|\rho^{\mathrm{TF}}_{1,\omega}\right\|_2^2 - 2\int_{\mathbb{R}^3}\mathrm{d}\vec{x}\,\varsigma\left|\phi^{\mathrm{GP}}_\omega\right|^2.$$

Additionally we need

$$\mathcal{E}^{\mathrm{TF}}_{1,\omega}\left[\left|\phi^{\mathrm{GP}}_\omega\right|^2\right] - \mu^{\mathrm{TF}}_{1,\omega} = \left\|\phi^{\mathrm{GP}}_\omega\right\|_4^4 - 2\int_{\mathbb{R}^3}\mathrm{d}\vec{x}\,\varsigma\left|\phi^{\mathrm{GP}}_\omega\right|^2$$

and by using (4.5) we conclude that

$$\int_{\mathbb{R}^3}\mathrm{d}\vec{x}\,\left(\left|\phi^{\mathrm{GP}}_\omega\right|^2 - \rho^{\mathrm{TF}}_{1,\omega}\right)^2 \leq \mathcal{E}^{\mathrm{TF}}_{1,\omega}\left[\left|\phi^{\mathrm{GP}}_\omega\right|^2\right] - E^{\mathrm{TF}}_{1,\omega} \leq g^{st/\sigma}E^{\mathrm{GP}}_{g,\Omega} - E^{\mathrm{TF}}_{1,\omega}.$$

The result is then obtained by applying Theorem 5.1.

□

5.2 The Electrostatic Analogy

In this section we adapt a result by Michele Correggi and Jakob Yngvason [CY08] for use in the proof of theorem 5.1. It will enable us to get an upper bound on the kinetic energy contribution of the vortex lattice to the value of the GP functionals (3.14) and (3.16) on a chosen trial function (5.2). In its proof we will follow the implications of a fascinating insight by Correggi and Yngavson. At its core is the analogy between the vortices' contribution to the kinetic energy and a problem from electrostatics. In this picture the vortices will assume the role of unit charges on a plane and the vector potential $\vec{A}_\omega$ (see (3.14)) will transform to an electric field of a uniform charge distribution. Our aim is to place the 'vortex' unit charges in a way such that their field cancel out the uniform field as far as possible. This will lead to the regular vortex pattern $\mathcal{L}_\varepsilon$ as defined in (5.7) and we will see that the dipole moments of the lattice cell will vanish — the essential idea of [CY08]. A more detailed description of the analogy can be found in the proof of the following proposition.

Proposition 5.3 (Electrostatic analogy) *Let the phase factor g_ε be defined as in* (5.10)*, $\rho \equiv \rho_{1,\omega}^{\mathrm{TF,2D}}$ as in* (5.28)*, the cut-off function χ_ε as in* (5.12) *and the vector potential $\vec{A}_{\omega/\varepsilon}$ be given by* (3.3) *and* (3.13)*; then*[7]

$$\int_{\mathcal{D}} \mathrm{d}\vec{r}\, \rho\, \chi_\varepsilon^2 \left| \left(\vec{\nabla} - i\vec{A}_{\omega/\varepsilon}\right) g_\varepsilon \right|^2 \leq \frac{\omega}{2} \frac{|\log \varepsilon|}{\varepsilon} + O(\varepsilon^{-1}) \tag{5.37}$$

with $\mathcal{D} \equiv \mathcal{S}_{2D} \cup \mathcal{O}_{2D}$ a subset of $\mathbb{R}^2$ defined in (5.20) *and* (5.21)*.*

Proof: As in (5.17) we have that

$$\left| \left(\vec{\nabla} - i\vec{A}_{\omega/\varepsilon}\right) g_\varepsilon \right|^2 = \left| \vec{\nabla}\theta_\varepsilon - \vec{A}_{\omega/\varepsilon} \right|^2$$

with θ_ε denoting the phase function of g_ε (see(5.11)). As a first step to establish the analogy we define with

$$\phi_\varepsilon(\vec{r}) = \sum_{\vec{r}_i \in \mathcal{L}_\varepsilon} \log|\vec{r} - \vec{r}_i|$$

the potential of the electric field of (two-dimensional) point charges located at the lattice centers $\vec{r}_i$, i.e.,

$$\vec{\nabla}\phi_\varepsilon(\vec{r}) = \sum_{\vec{r}_i \in \mathcal{L}_\varepsilon} \frac{\vec{r} - \vec{r}_i}{|\vec{r} - \vec{r}_i|^2}.$$

Note that we use scaled units such that $2\pi\epsilon_0 = 1$. It turns out that ϕ_ε is the conjugate harmonic function of our phase function θ_ε, i.e., $\partial_x\phi_\varepsilon = \partial_y\theta_\varepsilon$ and $\partial_y\phi_\varepsilon = -\partial_x\theta_\varepsilon$. This allows us to write

$$\left| \vec{\nabla}\theta_\varepsilon - \vec{A}_{\omega/\varepsilon} \right|^2 = \left| \begin{pmatrix} \partial_x\theta_\varepsilon \\ \partial_y\theta_\varepsilon \end{pmatrix} + \frac{\omega}{2\varepsilon} \begin{pmatrix} -y \\ x \end{pmatrix} \right|^2 = \left| \begin{pmatrix} -\partial_y\phi_\varepsilon \\ \partial_x\phi_\varepsilon \end{pmatrix} + \frac{\omega}{2\varepsilon} \begin{pmatrix} -y \\ x \end{pmatrix} \right|^2 = \left| \vec{\nabla}\phi_\varepsilon - \frac{\omega}{2\varepsilon}\vec{r} \right|^2$$

where $\omega/(2\varepsilon)\vec{r}$ can be seen as the electric field of a (two-dimensional) uniform charge distribution with density $\omega/(2\pi\varepsilon)$. Hence we define our imaginary electric field as

$$\vec{E}(\vec{r}) \equiv \vec{\nabla}\phi_\varepsilon(\vec{r}) - \frac{\omega}{2\varepsilon}\vec{r}$$

[7] Since all the used functions are defined on $\mathbb{R}^2$ we will denote with $\vec{\nabla}$ the *two*-dimensional gradient (∂_x, ∂_y).

which allows us to restate the goal of this proposition as the bound

$$\int_{\mathcal{D}} \mathrm{d}\vec{r}\, \rho\, \chi_{\underline{\varepsilon}}^2 \left|\vec{E}\right|^2 \leq \frac{\omega}{2} \frac{|\log \underline{\varepsilon}|}{\underline{\varepsilon}} + O(\underline{\varepsilon}^{-1}). \tag{5.38}$$

Later on we will partition the domain of integration into the lattice cells $Q_{\underline{\varepsilon}}^i$ and evaluate the integral on each one separately.

The potential of the electric field in cell $Q_{\underline{\varepsilon}}^i$ is given by

$$\Phi_i(\vec{r}\,) \equiv \int_{\mathcal{D}} \mathrm{d}\vec{r}\,'\, \sigma_i(\vec{r}\,')\log|\vec{r} - \vec{r}\,'|$$

with the charge density

$$\begin{aligned}\sigma_i(\vec{r}\,') &\equiv \delta(\vec{r}\,' - \vec{r}_i) - \frac{\omega}{2\pi\underline{\varepsilon}}\chi_i(\vec{r}\,') \\ &= \delta(\vec{r} - \vec{r}_i) - \left|Q_{\underline{\varepsilon}}^i\right|^{-1} \chi_i(\vec{r}\,')\end{aligned}$$

where χ_i is the characteristic function of the lattice cell $Q_{\underline{\varepsilon}}^i$ and $\delta(\cdot)$ the two-dimensional Dirac distribution. We see that the charge distribution of a single cell is neutral and we have chosen the size of a lattice cell (5.7) in a way such that $\vec{E}(\vec{r}\,) = \sum_{\vec{r}_i \in \mathcal{L}_{\underline{\varepsilon}}} \vec{\nabla}\Phi_i(\vec{r}\,) \equiv \vec{\nabla}\Phi(\vec{r}\,)$ holds. Through appliance of the coordinate transformation

$$\vec{r} = \underline{\varepsilon}^{1/2}\vec{\kappa} \tag{5.39}$$

the lattice scaling becomes independent of $\underline{\varepsilon}$ and we denote the new cells with Q_1^i. We use the same scaling on the various quantities we defined above and get

$$\sigma_i(\vec{r}\,') = \underline{\varepsilon}^{-1}\left(\delta(\vec{\kappa}' - \vec{\kappa}_i) - \left|Q_1^i\right|^{-1}\chi_{i,1}(\vec{\kappa}')\right) = \underline{\varepsilon}^{-1}\sigma_i(\vec{\kappa}') \tag{5.40}$$

as well as

$$\begin{aligned}\vec{E}_i(\vec{r}\,) &= \underline{\varepsilon}^{-1/2}\vec{E}_{i,1}(\vec{\kappa}) \\ &= \underline{\varepsilon}^{-1/2}\vec{\nabla}\Phi_{i,1}(\vec{\kappa}) = \vec{\nabla}\int_{\mathcal{D}} \mathrm{d}\vec{\kappa}'\, \sigma_{i,1}(\vec{\kappa}')\log|\vec{\kappa}' - \vec{\kappa}|\,.\end{aligned} \tag{5.41}$$

For a point $\vec{\kappa} \in Q_1^i$ we have two distinct contributions to the potential $\Phi_1(\vec{\kappa})$ — the potential $\Phi_{i,1}$ of its own cell and the contribution of all other cells' potentials. To estimate the latter quantity we can use our knowledge about the cells' shape and their charge density. Let Q_1^0 be a cell with its center at the origin — an assumption we make only for the sake of a more simple notation since the following observations can be transfered to arbitrary cells Q_1^i and $Q_{\underline{\varepsilon}}^i$ by translation and scaling. For points $\vec{\kappa} \notin Q_1^0$ we have the (cylindrical) multipole expansion of the associated potential $\Phi_{0,1}$ given by

$$\Phi_{0,1}(\vec{\kappa}) = q\log r - \sum_{m=1}^{\infty} \frac{C_m \cos m\theta + S_m \sin m\theta}{r^m}$$

with polar coordinates (r, θ). The multipole moments are defined as

$$q = \int_{Q_1^0} \mathrm{d}\vec{\kappa}\, \sigma_{0,1}(\vec{\kappa})$$

$$C_m = \frac{1}{m}\int_{Q_1^0} \mathrm{d}\vec{\kappa}\, \sigma_{0,1}(\vec{\kappa})\, r^m \cos m\theta$$

$$S_m = \frac{1}{m} \int_{Q_1^0} \mathrm{d}\vec{\kappa}\, \sigma_{0,1}(\vec{\kappa})\, r^m \sin m\theta.$$

From the neutral charge distribution (5.40) follows that the lowest moment vanishes, i.e. $q = 0$. Since we have assumed a regular lattice (see (5.7)) the dipole moments C_1 and S_1 evaluate to zero. This implies that the potential $\Phi_{0,1}$ is of order $O(r^{-2})$ or lower and that the electric field $\vec{E}_{0,1}$ decays at least as r^{-3}. We note that for square or hexagonal lattices even higher moments vanish and the decay is even faster. Mind that this conclusion is independent of $\underline{\varepsilon}$ due to the scaling (5.39).

We infer that if we have two distinct (unscaled) cells $Q_{\underline{\varepsilon}}^i$ and $Q_{\underline{\varepsilon}}^j$ with a mutual distance $O(\underline{\varepsilon}^{1/2}n)$, then the electric field of one cell, $\vec{E}_i$, evaluated at a point of the other cell, $\vec{r} \in Q_{\underline{\varepsilon}}^j$, is at most $O(\underline{\varepsilon}^{-1/2}n^{-3})$. This follows directly from the scalings (5.39) and (5.41). This allows us to estimate the contributions of all other cells $\bigcup_{j\neq i} Q_{\underline{\varepsilon}}^j$ to the electric field $\vec{E}(\vec{r})$ at points of the cell $Q_{\underline{\varepsilon}}^i$, namely, for $\vec{r} \in Q_{\underline{\varepsilon}}^i$ we obtain

$$\left|\vec{E}(\vec{r}) - \vec{E}_i(\vec{r})\right| \leq \sum_{j\neq i} \left|\vec{E}_j(\vec{r})\right| \leq O(\underline{\varepsilon}^{-1/2})$$

since the number of cells with distance $O(\underline{\varepsilon}^{1/2}n)$ from $Q_{\underline{\varepsilon}}^i$ is $O(n)$. We derive an upper bound on the electric field by the simple equality

$$\left|\vec{E}\right|^2 = \left|\vec{E}_i\right|^2 + 2\left(\vec{E} - \vec{E}_i\right) \cdot \vec{E}_i + \left|\vec{E} - \vec{E}_i\right|^2$$

and the observation that $\vec{E}_i(\vec{r}) \leq |\vec{r} - \vec{r}_i|^{-1}$ for $\vec{r} \in Q_{\underline{\varepsilon}}^i$ as

$$\left|\vec{E}(\vec{r})\right|^2 \leq \left|\vec{E}_i(\vec{r})\right|^2 + C_\omega \left(\underline{\varepsilon}^{-1/2} \left|\vec{r} - \vec{r}_i\right|^{-1} + \underline{\varepsilon}^{-1}\right). \tag{5.42}$$

Recalling our goal, the estimate of (5.38), we are able to split the integration into the respective contribution of the lattice cells, namely,

$$\begin{aligned}\int_{\mathcal{D}} \mathrm{d}\vec{r}\, \rho(\vec{r})\, \chi_{\underline{\varepsilon}}(\vec{r})^2 \left|\vec{E}(\vec{r})\right|^2 &\leq \sum_i \int_{Q_{\underline{\varepsilon}}^i} \mathrm{d}\vec{r}\, \rho(\vec{r})\, \chi_{\underline{\varepsilon}}(\vec{r})^2 \left|\vec{E}(\vec{r})\right|^2 \\ &\leq \sum_i \Big(\sup_{\vec{r}\,'\in Q_{\underline{\varepsilon}}^i} \rho(\vec{r}\,')\Big) \int_{Q_{\underline{\varepsilon}}^i} \mathrm{d}\vec{r}\, \chi_{\underline{\varepsilon}}(\vec{r})^2 \left|\vec{E}(\vec{r})\right|^2\end{aligned}$$

where the summation $\sum_i$ is meant to be taken over all lattice cells with centers at $\vec{r}_i \in \mathcal{L}_{\underline{\varepsilon}}$. In the right hand term we substituted the integration of the density over the lattice cells with its supremum in the respective cells; we will show later on that the errors such an approximation introduces are controllable. Denoting with $\mathcal{B}_{\underline{\varepsilon}}^i$ the disc with radius $\underline{\varepsilon}$ around $\vec{r}_i$ and adding the term $\left|\vec{E}_i\right|^2 - \left|\vec{E}_i\right|^2$ yields

$$\begin{aligned}&\sum_i \Big(\sup_{\vec{r}\,'\in Q_{\underline{\varepsilon}}^i} \rho(\vec{r}\,')\Big) \int_{Q_{\underline{\varepsilon}}^i} \mathrm{d}\vec{r}\, \chi_{\underline{\varepsilon}}(\vec{r})^2 \left|\vec{E}(\vec{r})\right|^2 \\ &\qquad = \sum_i \Big(\sup_{\vec{r}\,'\in Q_{\underline{\varepsilon}}^i} \rho(\vec{r}\,')\Big) \Bigg(\int_{Q_{\underline{\varepsilon}}^i \setminus \mathcal{B}_{\underline{\varepsilon}}^i} \mathrm{d}\vec{r}\, \left(\left|\vec{E}(\vec{r})\right|^2 - \left|\vec{E}_i(\vec{r})\right|^2\right) \\ &\qquad\qquad + \int_{\mathcal{B}_{\underline{\varepsilon}}^i} \mathrm{d}\vec{r}\, \chi_{\underline{\varepsilon}}(\vec{r})^2 \left(\left|\vec{E}(\vec{r})\right|^2 - \left|\vec{E}_i(\vec{r})\right|^2\right) \\ &\qquad\qquad + \int_{Q_{\underline{\varepsilon}}^i \setminus \mathcal{B}_{\underline{\varepsilon}}^i} \mathrm{d}\vec{r}\, \left|\vec{E}_i(\vec{r})\right|^2 + \int_{\mathcal{B}_{\underline{\varepsilon}}^i} \mathrm{d}\vec{r}\, \chi_{\underline{\varepsilon}}(\vec{r})^2 \left|\vec{E}_i(\vec{r})\right|^2 \Bigg)\end{aligned} \tag{5.43}$$

the integrals of which we will estimate separately. We have

$$\int_{Q^i_{\underline{\varepsilon}}\setminus\mathcal{B}^i_{\underline{\varepsilon}}} \mathrm{d}\vec{r}\,\left|\vec{E}_i(\vec{r})\right|^2 \leq 2\pi \int_{\underline{\varepsilon}}^{C_\omega \underline{\varepsilon}^{1/2}} \mathrm{d}r\, r\, r^{-2} = \pi\left|\log \underline{\varepsilon}\right| + O(1) \tag{5.44}$$

and

$$\int_{\mathcal{B}^i_{\underline{\varepsilon}}} \mathrm{d}\vec{r}\,\chi_{\underline{\varepsilon}}(\vec{r})^2\left|\vec{E}_i(\vec{r})\right|^2 \leq 2\pi \int_0^{\underline{\varepsilon}} \mathrm{d}r\, r\,\left(\frac{r}{\underline{\varepsilon}}\right)^2 r^{-2} = O(1).$$

From (5.42) follows that

$$\int_{Q^i_{\underline{\varepsilon}}\setminus\mathcal{B}^i_{\underline{\varepsilon}}} \mathrm{d}\vec{r}\,\left(\left|\vec{E}(\vec{r})\right|^2 - \left|\vec{E}_i(\vec{r})\right|^2\right) \leq C_\omega \int_{\underline{\varepsilon}}^{C_\omega \underline{\varepsilon}^{1/2}} \mathrm{d}r\, r\,\left(\underline{\varepsilon}^{-1/2} r^{-1} + \underline{\varepsilon}^{-1}\right) = O(1)$$

and

$$\int_{\mathcal{B}^i_{\underline{\varepsilon}}} \mathrm{d}\vec{r}\,\chi_{\underline{\varepsilon}}(\vec{r})^2\left(\left|\vec{E}(\vec{r})\right|^2 - \left|\vec{E}_i(\vec{r})\right|^2\right) \leq C_\omega \int_0^{\underline{\varepsilon}} \mathrm{d}r\, r\,\left(\frac{r}{\underline{\varepsilon}}\right)^2\left(\underline{\varepsilon}^{-1/2} r^{-1} + \underline{\varepsilon}^{-1}\right) = O(\underline{\varepsilon}^{1/2}).$$

To complete the estimate on (5.43) we have to bound the the error of the Riemann approximation

$$\mathcal{R} \equiv \left|Q^0_{\underline{\varepsilon}}\right| \sum_i \sup_{\vec{r}\in Q^i_{\underline{\varepsilon}}} \rho(\vec{r}) - \underbrace{\int_{\mathcal{D}} \mathrm{d}\vec{r}\,\rho(\vec{r})}_{=1 \text{ (see (5.28))}} \leq \left|Q^0_{\underline{\varepsilon}}\right| \sum_i \left(\sup_{\vec{r}\in Q^i_{\underline{\varepsilon}}} \rho(\vec{r}) - \inf_{\vec{r}\in Q^i_{\underline{\varepsilon}}} \rho(\vec{r})\right).$$

The difference between the supremum and infimum is of order $\underline{\varepsilon}^{1/2}$ since $\sup_{\vec{r}\in\mathcal{D}} \mathrm{d}\rho/\mathrm{d}r \leq C_\omega$ (see section 4.4.3) and the cell spacing is $O(\underline{\varepsilon}^{1/2})$ (see (5.8)). The number of cells is bounded by $C_\omega \underline{\varepsilon}^{-1}\left(1 + O(\underline{\varepsilon}^{1/2})\right)$ (see (5.9)) and thus we get

$$\mathcal{R} \leq C_\omega\, \underline{\varepsilon}\, \underline{\varepsilon}^{1/2}\, \underline{\varepsilon}^{-1}(1 + \underline{\varepsilon}^{1/2}) \leq \underline{\varepsilon}^{1/2}(1 + \underline{\varepsilon}^{1/2}).$$

Combining these results we can estimate the right hand side terms of (5.43) and arrive at

$$\int_{\mathcal{D}} \mathrm{d}\vec{r}\,\rho\,\chi^2_{\underline{\varepsilon}}\left|\vec{E}\right|^2 \leq \left|Q^0_{\underline{\varepsilon}}\right|^{-1}(\mathcal{R}+1)(\pi\left|\log \underline{\varepsilon}\right| + O(1)) \leq \frac{\omega}{2}\frac{\left|\log \underline{\varepsilon}\right|}{\underline{\varepsilon}} + O(\underline{\varepsilon}^{-1})$$

which completes the proof.

□

5.3 TF Limit for $\omega \to \infty$

In the regime of a dominating rotational energy contribution to the GP energy we have to take account of the fact that the TF density becomes highly concentrated in the limit of $g \to \infty$. An exact description of this behavior is given in lemma 4.1 and lemma 4.2. Furthermore we do not encounter a vortex lattice anymore but we see a giant vortex in its stead.

Theorem 5.4 (GP energy asymptotics for $\omega \to \infty$) *Using the notation and relations prepared in sections 3.3 and 4.1 we demand that $\omega \to \infty$ in the TF limit (i.e. $g \to \infty$). It then follows that the GP energy is asymptotically*

$$\Omega^{-2s/(s-2)} E^{\mathrm{GP}}_{g,\Omega} = E^{\mathrm{TF}}_{0,1} + \begin{cases} O\left(\Omega^{-4/3} + \gamma^{1/2}\right) & \text{if } s \geq t \wedge t \geq 2 \\ O\left(\Omega^{-2t/(t+1)} + \gamma^{t/(t+2)}\right) & \text{if } s \geq t \wedge t < 2 \\ O\left(\bar{\Omega}^{-4/3} + \gamma^{1/2}\right) & \text{if } s < t \end{cases} \tag{5.45}$$

with $\underset{\sim}{\Omega} \equiv \Omega^{(s+2)/(s-2)}$, $\bar{\Omega} \equiv \Omega^{s(t+2)/((s-2)t)}$ *and* $\gamma = \omega^{-(s-2)t/(s+(s+2)t)}$. *Note that with* $\omega \to \infty$ *in the TF limit we automatically get* $\Omega \to \infty$.

Proof:

The proof will mainly consist of the evaluation of the scaled GP functional on a suitable function to gain an upper bound on the asymptotic GP energy. Similarly to lemma 4.2 we will use a radially symmetric trial function of which the support becomes concentrated around the circle described in lemma 4.1. To compensate for the additional magnetic-kinetic term in the GP functional a complex phase will be needed.

The lower bound is gained by simply ignoring the kinetic term in (3.19) or (3.23), i.e.,

$$\Omega^{-2s/(s-2)} E^{\mathrm{GP}}_{g,\Omega} \geq E^{\mathrm{TF}}_{\gamma,1} \geq E^{\mathrm{TF}}_{0,1}$$

where we used lemma 4.2.

The trial function will be a modified variant of (4.23), namely[8],

$$\phi_{\tau,\Delta}(\vec{x}) \equiv \sqrt{\tilde{\rho}_\tau(\vec{x})} \exp\left\{ i \left[\frac{r_0^2 \Delta}{2} \right] \phi \right\} \tag{5.46}$$

where $[\cdot]$ denotes the integer part. The definitions of $\tilde{\rho}_\tau$ and r_0 are the same as in lemma 4.1 and lemma 4.2 with the additional requirement that $\left\| \vec{\nabla} \sqrt{f} \right\|_2 < \infty$. As in theorem 5.1 the relative magnitudes of the external potential's exponents s and t decide which of the scaled GP functionals (3.19) or (3.23) has to be used. The parameter Δ will then be chosen accordingly to be either $\underset{\sim}{\Omega}$ or $\bar{\Omega}^{\beta}$. The evaluation of both functionals on the trial function $\phi_{\tau,\Delta}$ is very similar in both cases; thus we show the explicit calculations only with the functional $\mathcal{E}^{\mathrm{GP}}_{\gamma,\underset{\sim}{\Omega}}$ (which corresponds to $s > t$) and note the differences to the second one. Note that this choice corresponds to $s > t$.

We have that

$$\underset{\sim}{\Omega}^{-2} \mathcal{E}^{\mathrm{GP}}_{\gamma,\underset{\sim}{\Omega}}[\phi_{\tau,\underset{\sim}{\Omega}}] = \underset{\sim}{\Omega}^{-2} \int_{\mathbb{R}^3} \mathrm{d}\vec{x} \left\{ \left| \left(\vec{\nabla}' - i \vec{A}_{\underset{\sim}{\Omega}} \right) \phi_{\tau,\underset{\sim}{\Omega}} \right|^2 \right\} + \mathcal{E}^{\mathrm{TF}}_{\gamma,1}[\tilde{\rho}_\tau] \tag{5.47}$$

with the scaled gradient $\vec{\nabla}' \equiv \vec{\nabla}_{\vec{r}} + \underset{\sim}{\Omega}^{-\alpha} \vec{\nabla}_z$. We have already shown in lemma 4.2 that the last term is bounded by $E^{\mathrm{TF}}_{0,1} + O\left(\tau^{\min(t,2)}\right) + O\left(\gamma \tau^{-2}\right)$. The magnetic-kinetic term evaluates to

$$\begin{aligned} &\underset{\sim}{\Omega}^{-2} \int_{\mathbb{R}^3} \mathrm{d}\vec{x} \left\{ \left| \left(\vec{\nabla}' - i \vec{A}_{\underset{\sim}{\Omega}} \right) \phi_{\tau,\underset{\sim}{\Omega}} \right|^2 \right\} \\ &\qquad = \underset{\sim}{\Omega}^{-2} \int_{\mathbb{R}^3} \mathrm{d}\vec{x} \left| \vec{\nabla}' \sqrt{\tilde{\rho}_\tau} \right|^2 + \underset{\sim}{\Omega}^{-2} \int_{\mathbb{R}^3} \mathrm{d}\vec{x} \left| \left(\vec{\nabla}' - i \vec{A}_{\underset{\sim}{\Omega}} \right) \exp\left\{ i \left[\frac{r_0^2 \underset{\sim}{\Omega}}{2} \right] \phi \right\} \right|^2 \tilde{\rho}_\tau \end{aligned}$$

and we can estimate the gradient of the TF density by

$$\underset{\sim}{\Omega}^{-2} \int_{\mathbb{R}^3} \mathrm{d}\vec{x} \left| \vec{\nabla}' \sqrt{\tilde{\rho}_\tau} \right|^2 \leq \underset{\sim}{\Omega}^{-2} \tau^{-1} \left\| \vec{\nabla} \sqrt{f} \right\|_2 = O\left(\underset{\sim}{\Omega}^{-2} \tau^{-1} \right). \tag{5.48}$$

Here we used that $\left| \vec{\nabla}' h \right| \leq \left| \vec{\nabla} h \right|$ for a differentiable function h since the scaling factor $\underset{\sim}{\Omega}^{-\alpha}$ vanishes as $\Omega \to \infty$. In the case of $s < t$ we would have used the scaling given by the functional $\dot{\mathcal{E}}^{\mathrm{GP}}_{\gamma,\bar{\Omega}}$ in (3.23) and $\Delta = \bar{\Omega}^{\beta}$ obtaining $\bar{\Omega}^{-\beta} \to 0$ in the limit $\Omega \to \infty$. A straightforward calculation of the second

[8] We use cylindrical coordinates and write $\vec{x} = (r, \phi, z)$.

term yields

$$\underline{\Omega}^{-2}\int_{\mathbb{R}^3}\mathrm{d}\vec{x}\,\left|\left(\vec{\nabla}'-i\vec{A}_{\underline{\Omega}}\right)\exp\left\{i\left[\frac{r_0^2\underline{\Omega}}{2}\right]\phi\right\}\right|^2\tilde{\rho}_\tau$$
$$\leq\Omega^{-2}\int_{\mathbb{R}^3}\mathrm{d}\vec{x}\,\underbrace{\left(\frac{1}{r}\left[\frac{r_0^2\underline{\Omega}}{2}\right]-\frac{\underline{\Omega}}{2}r\right)^2}_{\equiv K}\tilde{\rho}_\tau=O\left(\tau^2\right)+O\left(\underline{\Omega}^{-2}\right)+O\left(\tau\underline{\Omega}^{-1}\right)$$

where we expanded K into a Taylor series around the circle with radius r_0 and used the fact that the distance between the border of the support of $\tilde{\rho}_\tau$ and this circle is τ. The additional terms which arise by taking the integer part of the first term in the integrand vanish faster than the given orders as $\underline{\Omega}\to\infty$. In the same limit we observe that K tends to zero for $r=r_0$ which is the precise reason for our choice of Δ in the phase factor of $\phi_{\tau,\underline{\Omega}}$. In the case of $s<t$ we have to choose $\Delta=\bar{\Omega}^{\,\beta}$ to obtain the same results as it cancels the prefactor $\bar{\Omega}^{\,-\beta}$ in the functional $\dot{\mathcal{E}}^{\mathrm{GP}}_{\gamma,\bar{\Omega}}$. Having arrived at

$$\Omega^{-2s/(s-2)}E^{\mathrm{GP}}_{g,\Omega}\leq E^{\mathrm{TF}}_{0,1}+O\left(\tau^{\min(t,2)}\right)+O\left(\gamma\tau^{-2}\right)+O\left(\underline{\Omega}^{-2}\tau^{-1}\right)+O\left(\tau\underline{\Omega}^{-1}\right)\tag{5.49}$$

the choice of τ depends on the relative magnitudes of $\underline{\Omega}$ and γ. We optimize the error terms by equating the first three orders of the right hand side of (5.49). The last term, $O\left(\tau\underline{\Omega}^{-1}\right)$, will always be dominated by $O\left(\underline{\Omega}^{-2}\tau^{-1}\right)$ for our choices of τ.

If $t\geq 2$ and $\underline{\Omega}^{-1}\leq\gamma^{3/8}$ we chose $\tau\equiv\gamma^{1/4}$ and arrive at

$$\Omega^{-2s/(s-2)}E^{\mathrm{GP}}_{g,\Omega}\leq E^{\mathrm{TF}}_{0,1}+O\left(\gamma^{1/2}\right)$$

whereas for $\underline{\Omega}^{-1}>\gamma^{3/8}$ we demand that $\tau\equiv\underline{\Omega}^{-2/3}$ and get

$$\Omega^{-2s/(s-2)}E^{\mathrm{GP}}_{g,\Omega}\leq E^{\mathrm{TF}}_{0,1}+O\left(\underline{\Omega}^{-4/3}\right).$$

In the case of $t<2$ a similar procedure yields

$$\Omega^{-2s/(s-2)}E^{\mathrm{GP}}_{g,\Omega}\leq E^{\mathrm{TF}}_{0,1}+O\left(\gamma^{t/(t+2)}\right)\quad\text{for }\underline{\Omega}^{-1}\leq\gamma^{(t+1)/(2(t+2))}$$

and

$$\Omega^{-2s/(s-2)}E^{\mathrm{GP}}_{g,\Omega}\leq E^{\mathrm{TF}}_{0,1}+O\left(\underline{\Omega}^{-2t/(t+1)}\right)\quad\text{for }\underline{\Omega}^{-1}>\gamma^{(t+1)/(2(t+2))}$$

For $s<t$ the evaluation of $\dot{\mathcal{E}}^{\mathrm{GP}}_{\gamma,\bar{\Omega}}$ on the trial function yields an equivalent estimate to (5.49) with all occurrences of $\underline{\Omega}$ replaced by $\bar{\Omega}$. Thus the final choices of τ stay the same with the sole difference being the impossibility of the case $t<2$.

□

A Source code

In this section we supply the *Mathematica* source code which is used to generate the illustrations of the TF densities in section 4.6. The code has major differences for the cases $\omega < \infty$ and $\omega \to \infty$ as $g \to \infty$ and both version are given in the following subsections.

The code has been tested and used with *Mathematica 6* and runs if copied to a Notebook file (.nb). To generate the different graphs one has to enter the desired values for s, t, ω and g, resp. s, t and Ω. It is possible to set the range of the graphs manually and we supply the values we used in section 4.6.

A.1 $\omega < \infty$

```
\[Rho]\[Omega][r_, z_, s_, t_, \[Omega]_, \[Mu]\[Omega]_] :=
 1/2 (\[Mu]\[Omega] + 1/4 \[Omega]^2 r^2 - r^s - Abs[z]^t)

z1 = z /.
   Solve[\[Rho]\[Omega][r, z, s, t, \[Omega], \[Mu]\[Omega]] == 0,
     z][[1]] // Quiet

z\[Omega]1[r_, s_,
  t_, \[Omega]_, \[Mu]\[Omega]_] := (-r^s + \[Mu]\[Omega] + (
   r^2 \[Omega]^2)/4)^(1/t)

r\[Omega]1in[z_, s_, t_, \[Omega]_, \[Mu]\[Omega]_] :=
 Block[{zeros = Select[Chop /@
      (r /.
        NSolve[\[Rho]\[Omega][r, z, s, t, \[Omega], \[Mu]\[Omega]] ==
          0, r])
     , (Im@# == 0 && Re@# > 0) &]}
  , If[Length@zeros == 1, Null, Min@zeros]
  ]

r\[Omega]1out[z_, s_, t_, \[Omega]_, \[Mu]\[Omega]_] :=
 Max@Select[Chop /@
    (r /.
      NSolve[\[Rho]\[Omega][r, z, s, t, \[Omega], \[Mu]\[Omega]] == 0,
        r])
   , (Im@# == 0 && Re@# > 0) &]

2*Integrate[\[Rho]\[Omega][r, z, s, t, \[Omega], \[Mu]\[Omega]], {z,
     0, z\[Omega]1[r, s, t, \[Omega], \[Mu]\[Omega]]},
    Assumptions -> {Re[t] > -1, r >= 0}] //
  PowerExpand // FullSimplify

VolZ[r_, s_, t_, \[Omega]_, \[Mu]\[Omega]_] := (
 t (-r^s + \[Mu]\[Omega] + (r^2 \[Omega]^2)/4)^(1 + 1/t))/(1 + t)

Rout[s_, t_, \[Omega]_, \[Mu]\[Omega]_] :=
 Max@Select[
   Chop /@ (r /.
```

```
      NSolve[\[Rho]\[Omega][r, 0, s, t, \[Omega], \[Mu]\[Omega]] == 0,
        r])
   , (Im@# == 0 && Re@# >= 0) &]

Rin[s_, t_, \[Omega]_, \[Mu]\[Omega]_] :=
 With[{zeros = Select[
     Chop /@ (r /.
        NSolve[\[Rho]\[Omega][r, 0, s, t, \[Omega], \[Mu]\[Omega]] ==
          0, r])
     , (Im@# == 0 && Re@# >= 0) &]}
  , If[Length@zeros == 1, 0, Min@zeros]
  ]

Vol[s_, t_, \[Omega]_, \[Mu]\[Omega]_] :=
 2 \[Pi]*NIntegrate[VolZ[r, s, t, \[Omega], \[Mu]\[Omega]]*r
   , {r
    , Rin[s, t, \[Omega], \[Mu]\[Omega]],
    Rout[s, t, \[Omega], \[Mu]\[Omega]]}]

\!\(
\*SubscriptBox[\(\[PartialD]\), \(r\)]\ z1\)

RZmax[s_, t_, \[Omega]_, \[Mu]\[Omega]_] := Select[
   Chop /@ (r /. NSolve[\!\(
\*SubscriptBox[\(\[PartialD]\), \(r\)]\ \(z\[Omega]1[r, s,
          t, \[Omega], \[Mu]\[Omega]]\)\) == 0, r])
   , (Im@# == 0
      && Re@# > Rin[s, t, \[Omega], \[Mu]\[Omega]]
      && Re@# < Rout[s, t, \[Omega], \[Mu]\[Omega]]) &
   ][[1]]

Zmax[s_, t_, \[Omega]_, \[Mu]\[Omega]_] :=
 z\[Omega]1[RZmax[s, t, \[Omega], \[Mu]\[Omega]], s,
  t, \[Omega], \[Mu]\[Omega]]

\[Rho]\[Omega]Max[s_,
  t_, \[Omega]_, \[Mu]\[Omega]_] := \[Rho]\[Omega][
  RZmax[s, t, \[Omega], \[Mu]\[Omega]], 0, s,
  t, \[Omega], \[Mu]\[Omega]]

\[Mu][s_, t_, \[Omega]_] :=
 If[Vol[s, t, \[Omega], 0] > 1, \[Mu]Neg[s, t, \[Omega]], \[Mu]Pos[s,
   t, \[Omega]]]

\[Mu]PosNext[s_, t_, \[Omega]_, \[Mu]Last_] := \[Mu]Last/
  Vol[s, t, \[Omega], \[Mu]Last]

\[Mu]Pos[s_, t_, \[Omega]_] := Monitor[
   FixedPoint[\[Mu]PosNext[s, t, \[Omega], n = #] &, 1,
```

```
    SameTest -> (Abs[#1 - #2] < 1*^-5 &)]
   , n];

\[Mu]NegNext[s_, t_, \[Omega]_, \[Mu]Last_] :=
 Block[{\[Mu]NextMax = \[Mu]Last/2, \[Mu]NextMin = (\[Mu]Last -
     2 \[Rho]\[Omega]Max[s, t, \[Omega], 0])/2,
   V = Vol[s, t, \[Omega], \[Mu]Last]}
  , (-\[Mu]Last \[Mu]NextMax +
   V \[Mu]Last \[Mu]NextMin + \[Mu]NextMax \[Mu]NextMin -
   V \[Mu]NextMax \[Mu]NextMin)/((-1 + V) \[Mu]Last -
   V \[Mu]NextMax + \[Mu]NextMin)
  ]

\[Mu]Neg[s_, t_, \[Omega]_] := Monitor[
   FixedPoint[\[Mu]NegNext[s, t, \[Omega],
      n = #] &, -\[Rho]\[Omega]Max[s, t, \[Omega], 0] 0,
    SameTest -> (Abs[#1 - #2] < 1*^-8 &)]
   , n];

gst[g_, s_, t_] := g^((t - s)/(s + (s + 2) t))

Gst[g_, s_, t_] :=(*g^((s+2t)/(s+(s+2)t))**)gst[g, s, t]

Block[{s = 4, t = 8, \[Omega] = 2.3225928310183153`, \[Mu]\[Omega],
  Ri, Ro, Rm, Zm, \[Rho]m, g = 1}
 , \[Mu]\[Omega] = \[Mu][s, t, \[Omega]];
 Ri = Rin[s, t, \[Omega], \[Mu]\[Omega]];
 Ro = Rout[s, t, \[Omega], \[Mu]\[Omega]];
 Rm = RZmax[s, t, \[Omega], \[Mu]\[Omega]];
 Zm = Zmax[s, t, \[Omega], \[Mu]\[Omega]];
 \[Rho]m = \[Rho]\[Omega]Max[s, t, \[Omega], \[Mu]\[Omega]];
 Print["Inner Radius: ", Ri]; Print["Outer Radius: ", Ro];
 Print["Radius maximal Z: ", Rm];
 Print["Maximal Z: ", Zm/gst[g, s, t]];
 Print["Z prefactors: ", gst[g, s, t] // N];
 Print["Density prefactors: ", Gst[g, s, t] // N];
 Print["Largest Densities: ", Gst[g, s, t]*\[Rho]m];
 Print["Probability: ", Vol[s, t, \[Omega], \[Mu]\[Omega]]];
 Print["Chemical Potential: ", \[Mu]\[Omega]];

 Print@DensityPlot[
   Gst[g, s, t]*\[Rho]\[Omega][Abs[r], gst[g, s, t] *z, s,
     t, \[Omega], \[Mu]\[Omega]]
   , {r, -1.475519796771867`(*-1.1*Ro*), 1.475519796771867`(*1.1*
    Ro*)}
   , {z, -1.0002367852634897`(*-1.1*Zm/gst[g,s,t]*),
    1.0002367852634897`(*1.1*Zm/gst[g,s,t]*)}
   , PlotRange -> {0, 1.1 Gst[g, s, t]*\[Rho]m}
   , ColorFunction ->
```

```
    Function[f,
     Blend[{{0, GrayLevel[0.92]}, {0.3301944449975971`(*Gst[g,s,
        t]*\[Rho]m*), Black}}, f]]
   , ColorFunctionScaling -> False
   , MeshFunctions -> {#3 &},
   Mesh -> {{{0, Directive[Black, Thick, Opacity[1]]}}}
   , FrameLabel -> {{Style["z", Black, Plain, Bold,
       FontSize -> Medium], None}
     , {Style["r", Black, Plain, Bold, FontSize -> Medium], None}}
   , RotateLabel -> False, Ticks -> Automatic, Axes -> True
   , MaxRecursion -> 15, PlotPoints -> 200, WorkingPrecision -> 50];
 1.1*Zm/gst[g, s, t]
]
```

A.2 $\omega \to \infty$

```
\[Rho]\[Gamma][r_, z_, s_, t_, \[Gamma]_, \[Mu]\[Gamma]_] :=
 1/(2 \[Gamma]) (\[Mu]\[Gamma] + 1/4 r^2 - r^s - Abs[z]^t)

z1 = z /.
   Solve[\[Rho]\[Gamma][r, z, s, t, \[Gamma], \[Mu]\[Gamma]] == 0,
     z][[2]] // Quiet

z\[Gamma]1[r_, s_,
  t_, \[Gamma]_, \[Mu]\[Gamma]_] := (r^2/4 - r^
   s + \[Mu]\[Gamma])^(1/t)

2*Integrate[\[Rho]\[Gamma][r, z, s, t, \[Gamma], \[Mu]\[Gamma]], {z,
     0, z\[Gamma]1[r, s, t, \[Gamma], \[Mu]\[Gamma]]},
    Assumptions -> {Re[t] > -1, r >= 0}] //
  PowerExpand // FullSimplify

VolZ[r_, s_, t_, \[Gamma]_, \[Mu]\[Gamma]_] := (
 t (r^2/4 - r^s + \[Mu]\[Gamma])^(1 + 1/t))/((1 + t) \[Gamma])

Rout[s_, t_, \[Gamma]_, \[Mu]\[Gamma]_] :=
 Max@Select[
   Chop /@ (r /.
      NSolve[\[Rho]\[Gamma][r, 0, s, t, \[Gamma], \[Mu]\[Gamma]] ==
        0])
   , (Im@# == 0 && Re@# >= 0) &]

Rin[s_, t_, \[Gamma]_, \[Mu]\[Gamma]_] :=
 With[{zeros = Select[
     Chop /@ (r /.
        NSolve[\[Rho]\[Gamma][r, 0, s, t, \[Gamma], \[Mu]\[Gamma]] ==
          0, r])
     , (Im@# == 0 && Re@# >= 0) &]}
  , If[Length@zeros == 1, 0, Min@zeros]
  ]
```

```
Vol[s_, t_, \[Gamma]_, \[Mu]\[Gamma]_] :=
 2 \[Pi]*NIntegrate[VolZ[r, s, t, \[Gamma], \[Mu]\[Gamma]]*r
   , {r
    , Rin[s, t, \[Gamma], \[Mu]\[Gamma]],
    Rout[s, t, \[Gamma], \[Mu]\[Gamma]]}]

\!\(
\*SubscriptBox[\(\[PartialD]\), \(r\)]\ z1\)

RZmax[s_, t_, \[Gamma]_, \[Mu]\[Gamma]_] := Select[
   Chop /@ (r /. NSolve[\!\(
\*SubscriptBox[\(\[PartialD]\), \(r\)]\ \(z\[Gamma]1[r, s,
          t, \[Gamma], \[Mu]\[Gamma]]\)\) == 0, r])
   , (Im@# == 0
      && Re@# > Rin[s, t, \[Gamma], \[Mu]\[Gamma]]
      && Re@# < Rout[s, t, \[Gamma], \[Mu]\[Gamma]]) &
   ][[1]]

Zmax[s_, t_, \[Gamma]_, \[Mu]\[Gamma]_] :=
 z\[Gamma]1[RZmax[s, t, \[Gamma], \[Mu]\[Gamma]], s,
  t, \[Gamma], \[Mu]\[Gamma]]

\[Rho]\[Gamma]Max[s_,
  t_, \[Gamma]_, \[Mu]\[Gamma]_] := \[Rho]\[Gamma][
  RZmax[s, t, \[Gamma], \[Mu]\[Gamma]], 0, s,
  t, \[Gamma], \[Mu]\[Gamma]]

\[Mu][s_, t_, \[Gamma]_] :=
 If[Vol[s, t, \[Gamma], 0] > 1, \[Mu]Neg[s, t, \[Gamma]], \[Mu]Pos[s,
   t, \[Gamma]]]

\[Mu]PosNext[s_, t_, \[Gamma]_, \[Mu]Last_] := \[Mu]Last/
  Vol[s, t, \[Gamma], \[Mu]Last]

\[Mu]Pos[s_, t_, \[Gamma]_] := Monitor[
   FixedPoint[\[Mu]PosNext[s, t, \[Gamma], n = #] &, 1,
    SameTest -> (Abs[#1 - #2] < 1*^-5 &)]
   , n];

\[Mu]NegNext[s_, t_, \[Gamma]_, \[Mu]Last_] :=
 Block[{\[Mu]NextMax = \[Mu]Last/2, \[Mu]NextMin = (\[Mu]Last -
     2 \[Gamma] \[Rho]\[Gamma]Max[s, t, \[Gamma], 0])/2,
   V = Vol[s, t, \[Gamma], \[Mu]Last]}
  , (-\[Mu]Last \[Mu]NextMax +
     V \[Mu]Last \[Mu]NextMin + \[Mu]NextMax \[Mu]NextMin -
     V \[Mu]NextMax \[Mu]NextMin)/((-1 + V) \[Mu]Last -
     V \[Mu]NextMax + \[Mu]NextMin)
  ]
```

```
\[Mu]Neg[s_, t_, \[Gamma]_] := Monitor[
   FixedPoint[\[Mu]NegNext[s, t, \[Gamma],
      n = #] &, -\[Gamma] \[Rho]\[Gamma]Max[s, t, \[Gamma], 0],
    SameTest -> (Abs[#1 - #2] < 1*^-8 &)]
   , n];

\[CapitalOmega]st[\[CapitalOmega]_, s_, t_] := \[CapitalOmega]^((
 2 (s - t))/((s - 2) t))

Block[{s = 6, t = 10, \[Gamma], \[Mu]\[Gamma], Ri, Ro, Rm,
  Zm, \[Rho]m, g, \[CapitalOmega] = 100}
 , g = 1*Sqrt[\[CapitalOmega]^((2 (s + (2 + s) t))/((-2 + s) t))];
 \[Gamma] = g \[CapitalOmega]^(-((2 (s + (s + 2) t))/((s - 2) t)));
 \[Mu]\[Gamma] = \[Mu][s, t, \[Gamma]];
 Ri = Rin[s, t, \[Gamma], \[Mu]\[Gamma]];
 Ro = Rout[s, t, \[Gamma], \[Mu]\[Gamma]];
 Rm = RZmax[s, t, \[Gamma], \[Mu]\[Gamma]];
 Zm = Zmax[s, t, \[Gamma], \[Mu]\[Gamma]];
 \[Rho]m = \[Rho]\[Gamma]Max[s, t, \[Gamma], \[Mu]\[Gamma]];
 Print["\[Gamma] : ", \[Gamma] // N];
 Print["Inner Radius: ", Ri]; Print["Outer Radius: ", Ro];
 Print["Radius maximal Z: ", Rm];
 Print["Maximal Z: ", Zm/\[CapitalOmega]st[\[CapitalOmega], s, t]];
 Print["Z prefactors: ", \[CapitalOmega]st[\[CapitalOmega], s, t] //
   N];
 Print["Density prefactors: ", \[CapitalOmega]st[\[CapitalOmega], s,
    t] // N];
 Print["Largest Densities: ", \[CapitalOmega]st[\[CapitalOmega], s,
    t]*\[Rho]m];
 Print["Probability: ", Vol[s, t, \[Gamma], \[Mu]\[Gamma]]];
 Print["Chemical Potential: ", \[Mu]\[Gamma]];

 Print@DensityPlot[
   \[CapitalOmega]st[\[CapitalOmega], s, t]*\[Rho]\[Gamma][
     Abs[r], \[CapitalOmega]st[\[CapitalOmega], s, t] *z, s,
     t, \[Gamma], \[Mu]\[Gamma]]
   , {r, -1.0398358728215993`(*-1.1*Ro*), 1.0398358728215993`(*1.1*
    Ro*)}
   , {z, -2.668560649906518`(*-1.1*
    Zm/\[CapitalOmega]st[\[CapitalOmega],s,t]*),
    2.668560649906518`(*1.1*Zm/\[CapitalOmega]st[\[CapitalOmega],s,
    t]*)}
   , PlotRange -> {0,
     1.1*\[CapitalOmega]st[\[CapitalOmega], s, t]*\[Rho]m}
   , ColorFunction ->
    Function[f,
     Blend[{{0,
        GrayLevel[
```

```
        0.92]}, {\[CapitalOmega]st[\[CapitalOmega], s, t]*\[Rho]m,
       Black}}, f]]
   , ColorFunctionScaling -> False
   , MeshFunctions -> {#3 &},
   Mesh -> {{{0, Directive[Black, Thick, Opacity[1]]}}}
   , FrameLabel -> {{Style["z", Black, Plain, Bold,
       FontSize -> Medium], None}
     , {Style["r", Black, Plain, Bold, FontSize -> Medium], None}}
   , RotateLabel -> False, Ticks -> Automatic, Axes -> True
   (*,MaxRecursion->15,PlotPoints->200,WorkingPrecision->50*)
   , MaxRecursion -> 5, PlotPoints -> 100, WorkingPrecision -> 50];
 Zm/\[CapitalOmega]st[\[CapitalOmega], s, t]
]
```

B Acknowledgments

I would like to express my gratitude to my supervisor, Prof. Dr. Jakob Yngvason, whose expertise and patience were very helpful and enlightening during my studies and the writing this thesis. Furthermore I thank my parents for their financial support and JB for her helpful hints.

References

[AEM+95] M. H. Anderson, J. R. Ensher, M. R. Matthews, C. E. Wieman, and E. A. Cornell. Observation of Bose-Einstein Condensation in a Dilute Atomic Vapor. *Science*, 269:198–201, July 1995.

[Aft07] A. Aftalion. *Vortices in Bose-Einstein condensates*. Progress in nonlinear differential equations and their applications. Birkhauser, Boston, MA, 2007.

[AM38] J. F. Allen and A. D. Misener. Flow of Liquid Helium II. *Nature*, 141:75, January 1938.

[ARVK01] J. R. Abo-Shaeer, C. Raman, J. M. Vogels, and W. Ketterle. Observation of Vortex Lattices in Bose-Einstein Condensates. *Science*, 292:476–479, April 2001.

[BCPY08] J.-B. Bru, M. Correggi, P. Pickl, and J. Yngvason. The TF Limit for Rapidly Rotating Bose Gases in Anharmonic Traps. *Communications in Mathematical Physics*, 280:517–544, June 2008.

[Bog47a] N. N. Bogoliubov. On the Theory of Superfluidity. *Izv. Academii Nauk USSR*, 11(1):77, 1947.

[Bog47b] N. N. Bogoliubov. On the Theory of Superfluidity. *Journal of Physics*, 11(1):23–32, 1947.

[Bos24] S. N. Bose. Plancks Gesetz und Lichtquantenhypothese. *Zeitschrift fur Physik*, 26:178–181, December 1924.

[CMD00] F. Chevy, K. W. Madison, and J. Dalibard. Measurement of the Angular Momentum of a Rotating Bose-Einstein Condensate. *Physical Review Letters*, 85:2223–2227, September 2000.

[Coo08] N. R. Cooper. Rapidly rotating atomic gases. *Advances in Physics*, 57:539–616, November 2008.

[CRDY07a] M. Correggi, T. Rindler-Daller, and J. Yngvason. Rapidly rotating Bose-Einstein condensates in homogeneous traps. *Journal of Mathematical Physics*, 48(10):102103, 2007.

[CRDY07b] M. Correggi, T. Rindler-Daller, and J. Yngvason. Rapidly rotating Bose-Einstein condensates in strongly anharmonic traps. *Journal of Mathematical Physics*, 48(4):042104, 2007.

[CW02] E. A. Cornell and C. E. Wieman. Nobel Lecture: Bose-Einstein condensation in a dilute gas, the first 70 years and some recent experiments. *Reviews of Modern Physics*, 74:875–893, August 2002.

[CY08] M. Correggi and J. Yngvason. Energy and vorticity in fast rotating Bose-Einstein condensates. *Journal of Physics A: Mathematical and Theoretical*, 41(44):445002 (19pp), 2008.

[DGPS99] F. Dalfovo, S. Giorgini, L. P. Pitaevskii, and S. Stringari. Theory of Bose-Einstein condensation in trapped gases. *Reviews of Modern Physics*, 71:463–512, April 1999.

[DMA+95] K. B. Davis, M.-O. Mewes, M. R. Andrews, N. J. van Druten, D. S. Durfee, D. M. Kurn, and W. Ketterle. Bose-Einstein condensation in a gas of sodium atoms. *Physical Review Letters*, 75:3969–3973, November 1995.

[Ein25] A. Einstein. Quantentheorie des einatomigen idealen Gases (Zweite Abhandlung). *Sitzungsber. Kgl. Preuss. Akad. Wiss.*, 1925.

[Fet09] A. L. Fetter. Rotating trapped Bose-Einstein condensates. *Reviews of Modern Physics*, 81:647–691, April 2009.

[GRJ03] M. Greiner, C. A. Regal, and D. S. Jin. Emergence of a molecular Bose-Einstein condensate from a Fermi gas. *Nature*, 426:537–540, December 2003.

[Gro61] E. P. Gross. Structure of a quantized vortex in boson systems. *Il Nuovo Cimento*, 20(3):454–477, May 1961.

[Gro63] E. P. Gross. Hydrodynamics of a Superfluid Condensate. *Journal of Mathematical Physics*, 4:195–207, February 1963.

[HHDB99] L. V. Hau, S. E. Harris, Z. Dutton, and C. H. Behroozi. Light speed reduction to 17 metres per second in an ultracold atomic gas. *Nature*, 397:594–598, February 1999.

[JBA+03] S. Jochim, M. Bartenstein, A. Altmeyer, G. Hendl, S. Riedl, C. Chin, J. Hecker Denschlag, and R. Grimm. Bose-Einstein Condensation of Molecules. *Science*, 302:2101–2104, December 2003.

[Kap38] P. Kapitza. Viscosity of Liquid Helium below the λ-Point. *Nature*, 141:74, January 1938.

[Ket02] W. Ketterle. Nobel lecture: When atoms behave as waves: Bose-Einstein condensation and the atom laser. *Reviews of Modern Physics*, 74:1131–1151, November 2002.

[LDBH01] C. Liu, Z. Dutton, C. H. Behroozi, and L. V. Hau. Observation of coherent optical information storage in an atomic medium using halted light pulses. *Nature*, 409:490–493, January 2001.

[LIB+09] O. Lahav, A. Itah, A. Blumkin, C. Gordon, and J. Steinhauer. A sonic black hole in a density-inverted Bose-Einstein condensate. *ArXiv e-prints*, June 2009.

[Lon38] F. London. The λ-Phenomenon of Liquid Helium and the Bose-Einstein Degeneracy. *Nature*, 141:643–644, April 1938.

[LS02] E. H. Lieb and R. Seiringer. Proof of Bose-Einstein Condensation for Dilute Trapped Gases. *Physical Review Letters*, 88(17):170409, April 2002.

[LS06] E. H. Lieb and R. Seiringer. Derivation of the Gross-Pitaevskii Equation for Rotating Bose Gases. *Communications in Mathematical Physics*, 264:505–537, June 2006.

[LSY00] E. H. Lieb, R. Seiringer, and J. Yngvason. Bosons in a trap: A rigorous derivation of the Gross-Pitaevskii energy functional. *Physical Review A*, 61(4):043602, April 2000.

[MAH+99] M. R. Matthews, B. P. Anderson, P. C. Haljan, D. S. Hall, C. E. Wieman, and E. A. Cornell. Vortices in a bose-einstein condensate. *Phys. Rev. Lett.*, 83(13):2498–2501, Sep 1999.

[MCWD00] K. W. Madison, F. Chevy, W. Wohlleben, and J. Dalibard. Vortex Formation in a Stirred Bose-Einstein Condensate. *Physical Review Letters*, 84:806–809, January 2000.

[MP09] Jean Macher and Renaud Parentani. Black-hole radiation in bose-einstein condensates. *Phys. Rev. A*, 80(4):043601, Oct 2009.

[Pit61] L. P. Pitaevskii. Vortex Lines in an Imperfect Bose Gas. *Soviet Physics J. Experimental and Theoretical Physics*, 13:451–454, 1961.

[PO56] O. Penrose and L. Onsager. Bose-Einstein Condensation and Liquid Helium. *Physical Review*, 104:576–584, November 1956.

[RCC+01] J. L. Roberts, N. R. Claussen, S. L. Cornish, E. A. Donley, E. A. Cornell, and C. E. Wieman. Controlled Collapse of a Bose-Einstein Condensate. *Physical Review Letters*, 86:4211–4214, May 2001.

[SS95] W. M. Snow and P. E. Sokol. Density and temperature dependence of the momentum distribution in liquid helium 4. *Journal of Low Temperature Physics*, 101:881–928, December 1995.

Curriculum Vitae

Thomas Auzinger, geboren am 24. Jänner 1982 in Wien

1988 - 1992	Volksschule Gramatneusiedl
1992 - 2000	AHS Neulandschule, Wien (Abschluß mit Matura)
2000 - 2001	Wehrdienst
2001 -	Diplomstudium Mathematik
2001 - 2009	Diplomstudium Physik (Ummeldung auf Bachelor-, Masterstudium)
2009 - 2010	Bachelorstudium Physik (Abschluß mit Auszeichnung)
2010 -	Masterstudium Physik

(alle Studien an der Universität Wien)